AD-A055 636 AIR FORCE INST OF TECH WRIGHT-PATTERSON AFB OHIO SCH--ETC F/G 9/2
AN AUTOMATIC MAGNETIC BUBBLE MOBILITY MEASUREMENT SYSTEM EMPLOY--ETC(U)
MAR 78 R L EILERS

UNCLASSIFIED AFIT/GE/EE/78-1 NL

1 OF 1
ADA
055636

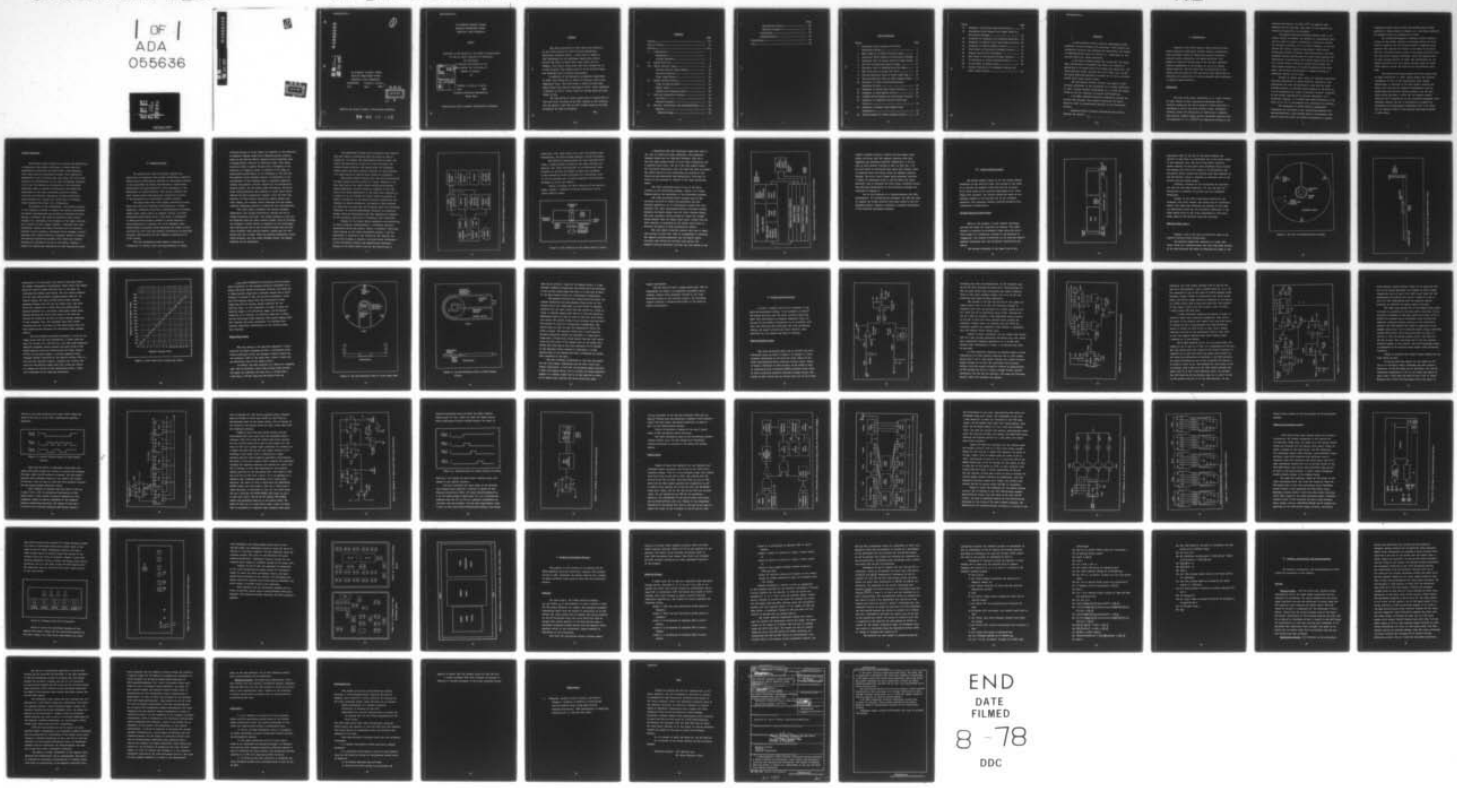

END
DATE
FILMED
8-78
DDC

AFIT/GE/EE/78-1

AN AUTOMATIC MAGNETIC BUBBLE MOBILITY MEASUREMENT SYSTEM EMPLOYING VIDEO PROCESSING

AFIT/GE/EE/78-1 Richard L. Eilers Capt USAF

Approved for public release; distribution unlimited

AFIT/GE/EE/78-1

AN AUTOMATIC MAGNETIC BUBBLE MOBILITY MEASUREMENT SYSTEM EMPLOYING VIDEO PROCESSING

THESIS

Presented to the Faculty of the School of Engineering
of the Air Force Institute of Technology
Air University
in Partial Fulfillment of the
Requirements for the Degree of
Master of Science
by

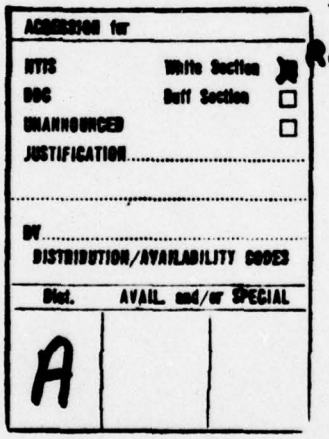

Richard L. Eilers, B.S.E.E.
Capt USAF
Graduate Electrical Engineering

March 1978

Approved for public release; distribution unlimited

Preface

The effort described in this report was sponsored by the United States Air Force Avionics Laboratory, Electronics Reaserch Branch. I would like to thank Dr. John Blasingame for his assistance during this effort. Without the likes of Harry Beck, Mike Globe, and Joe Omaggio, this report would never have been written due to a lack of parts. The support given to me by the AFIT shops was tremendous and is greatly appreciated.

In addition to fulfilling the graduation requirement at AFIT, this thesis was an effort at filling a void in my experience level. This tack would probably not have been taken without the help and teachings of Prof. Jerzy Lubelfeld. I consider my life a little richer for having known and been taught by him.

The last person to whom a great deal of thanks (and in this case love) is given is my wife. Because of her worrying over my thesis, I was free to work without doing so and thus accomplish the task on schedule.

RLE

Contents

		Page
Preface		iii
List of Figures		vi
Abstract		viii
I.	Introduction	1
	Background	1
	Problem Statement	4
II.	System Overview	5
III.	Bubble Mobility Stage	13
	Initial Mobility Stage Design	13
	Mobility Stage-Mod 1	15
	Final Stage Design	20
IV.	System and Electronics	25
	Video Processing Board	25
	Memory Board	38
	Chassis and Component Layout	44
V.	Mobility Computation Program	51
	Overview	51
	Mobility Program	52
VI.	Results, Conclusions, and Recommendations	58
	Results	58
	Mobility Stage	58

Page

Electronics Section..... 58

Mobility Program..... 62

Conclusions..... 62

Recommendations..... 63

Bibliography..... 65

Vita 66

List of Figures

Figure		Page
1	Functional Block Diagram of Mobility Measurement System.....	8
2	Basic Make-up of Bubble Mobility Stage.....	9
3	Functional Block Diagram of Electronics Package.	11
4	Elevation View of Initial Mobility Stage Design.	14
5	Top View of Modified Mobility Stage.....	16
6	Elevation View of Modified Mobility Stage.....	17
7	Bias Field Coil H versus VDC Curve.....	19
8	Top and Elevation Views of Final Stage Base.....	21
9	Top and Elevation Views of Brass Sample Holder..	22
10	Schematic of Video Discrimination/Level Detection Circuit.....	26
11	Schematic of Bubble Time Filter Section.....	28
12	Schematic of Data Enable Circuit.....	30
13	Overall Timing Diagram for Data Enable Circuit..	32
14	Schematic of Temporal Position Generating Circuit.....	33
15	Schematic of Memory Board Enable Pulse Generators.....	35
16	Timing Diagram for Memory Enable Circuit.....	36

Figure		Page
17	Schematic of Mobility Stage Electronics.....	37
18	Functional Block Diagram with Signal Paths for Electronics Package.....	39
19	Schematic of Temporary and Permanent Memories..	40
20	Schematic of Address Count and Display Circuit.	42
21	Schematic of Memory Display Circuit.....	43
22	Front Panel of Electronics Package Cabinet.....	45
23	Display Board Device Placement.....	46
24	Rear Panel of Electronics Package Cabinet.....	47
25	IC Placement on Video Processing Board.....	49
26	IC Placement on Memory Board.....	49
27	Cabinet Placement of Processing, Memory, and Power Supply Boards.....	50

Abstract

A semi-automatic bubble mobility measurement system employing a Zeiss Ultraplot 3B microscope, video camera, and processing circuitry was designed and constructed. The method of measurement was static in nature i.e. measurement of the pre and post-drive domain positions.

A two piece mobility stage was constructed. The stage base incorporated a removable bias field coil capable of generating a 160 gauss field with little heat generation. The brass specimen holder contains the drive field coil. An E&H 123 pulse generator/amplifier provides the 50 volt, one microsecond drive field current pulse.

The electronics section converts the domain's light contrast difference in the microscope to a voltage difference in time. Voltage contrast differences of 0.7 volts and domain widths of 2us are required to achieve discrimination.

A HP 9825 compatible mobility computation program was written and debugged. This program calculates the domain mobility based on displacement measured by the electronics section.

Simulated domain contrast differences were used to validate the system.

I. Introduction

Important rare earth magnetic garnet material parameters requiring measurement include material composition, film thickness, number of defects per square centimeter, material static properties, and domain mobility. With regard to practical devices one of the two most important material parameters is the domain, or, as it is called, bubble mobility. Device access time is determined by the bubble size and mobility. The purpose of this thesis was to determine the feasibility of using automated video techniques to measure bubble mobility.

Background

The rare earth garnet technology is of recent vintage. In 1968, Bobeck at Bell Laboratories announced device concepts suggesting the use of magnetic bubble materials in simulating a serial disk data storage system. Subsequent research proved the feasibility of fabrication a modestly high density magnetic memory device (presently memories with bit densities of $2.5 \times 10^6/in^2$ are undergoing testing at the

Avionics Laboratory). By 1985, 10^{12} bit magnetic mass memories with an intrinsic data rate of 0.78 megabits per second are expected to be available.

The Bubble Materials Technology Branch (DHR) is at present unable to monitor the validity of contractors' data due to a lack of in-house capability. A series of efforts are currently underway, mostly by AFIT students, to develop systems for bubble parameter measurement. Video signal processing, spatial filtering, spectrophotometry, and glow discharge optical spectroscopy are areas being explored for feasibility of application. This thesis deals with the use of a closed circuit television system (CCTV system) and video signal processing to provide information from which rapid and accurate calculations of domain mobility in materials' samples can be made.

Because of domain size, there are problems associated with the measurement of bubble mobility. Inherent in the requirement for high bit densities is the need for small storage elements. At present bubble domains on the order of 4 to 6 micrometers are found in practical devices. Available at the Avionic Laboratory are devices employing 1 to 2 micrometer domains. It is hoped that domain diameters on the order of 0.1 to 0.5 micrometers will eventually be achieved.

Two categories of bubble mobility measurement techniques are currently in use: optical/photographic and optical/electronic. Both methods employ a microscope. Both require polarized light for sample illumination to exploit

a magneto-optical effect called the Faraday Effect. These methods are mainly static in nature i.e., the domain positions are measured while the domains are at rest.

The optical/photographic technique involves taking a picture of the domain through a microscope before the drive field is applied. The drive field creates a magnetic field gradient that propels the bubbles at an angle to the field and at a velocity (cm/sec) equal to the domain mobility times the bias field strength (oersteds). After the domains come to rest, another picture is taken. The displacement of the domains divided by the bias field strength times the drive field duration yields the mobility for the material under test.

The second method approximates the first except that an image intensifier or video camera gathers the contrast information in lieu of the photographic film. Domain displacement is measured in the time domain. Knowing the raster scan rate and the temporal displacement found by subtracting the pre-drive bubble position from the post-drive bubble position, a value for the material domain mobility can be computed as in the preceeding paragraph. This technique employs the use of electronics in signal discrimination and displacement computation and is the basis for the approach taken in the mobility measurement system in this study.

Problem Statement

The problem simply stated is to explore the feasibility of employing video signal processing in domain mobility measurement by designing and fabricating a semi-automatic CCTV bubble mobility measurement system. This feasibility demonstration can be divided into four tasks. The first task involves the determination of the video processing technique (s) to use. The design and fabrication of the microscope mechanical stage is another problem area. The design and fabrication of the video processing circuitry, memory circuitry, and mobility computation program constitute a third problem area. Finally the system must be evaluated using simulated and actual video information.

In addition to the introduction, this thesis consists of five chapters. Chapter 2 contains the system requirements and design considerations and provides a subsystem overview. Chapter 3 discusses the mobility mechanical stage design. Included is a discussion with diagrams of the stage evolution from initial to final design. Chapter 4 describes the video processing, timing, and memory circuitry and its function. Detailed circuit analysis, functional block diagrams, circuit diagrams, and a board layout are included. Chapter 5 details the mobility computation program. Flow charts and computer listings are included as an aid to the reader. Chapter 6 states the results and conclusions of this feasibility study.

II. System Overview

The problem this report describes concerns the feasibility of employing video signal processing in magnetic domain mobility measurement. Inherent in the problem solution is the requirement to design and fabricate a system which demonstrates the applicability of video techniques to the measurement of bubble mobility. This section presents the major system design considerations including an overview of the subsystems to be discussed in later sections.

The requirement that video signal processing be used stems from some very important considerations. A system employing a completely electronic scanning/signal processing scheme lends itself easily to computer control. To permit statistical description (with a high level of confidence) of domain mobility within a sample of garnet material a large population is required. Use of an automated video camera/signal processing system maximizes the number of data collected per unit time and operator interaction. An important practical consideration was the immediate availability of a CCTV system.

The thin epitaxially grown layers of garnet are transparent to visible light. The applicability of visual

contrast devices (a video camera for example) to the detection of magnetic domains stems from a magneto-optical property known as the Faraday Effect. Magnetic garnet materials show a Faraday Effect rotation to polarized light. When plane-polarized light is passed through such a substance in the presence of a magnetic field, a rotation of the plane of polarization proportional to the thickness of the film and the magnetic field strength results. By adjustment of the polarization of the incoming light, a contrast difference between the parallel (bubble) domains and the antiparallel domains arises. For the system under discussion, the microscope cross-polarizers were adjusted to yield light bubble domains and dark antiparallel domains. Given the best combination of light source, microscope optical system, and video camera, the voltage levels resulting from the domain contrast differences should be sufficient for discrimination.

The video camera transforms the optical contrast differences into voltage differences. Through the use of signal processing circuitry, the bubble position in time can be extracted from the video contrast signal. Then by limiting the distance a bubble domain is displaced by the field gradient (through the use of short duration pulses and low bias field strength) easy pairing between a domain and its displaced self can be made. Using the position difference, drive field duration, and bias field strength values, the domain mobility can be calculated.

Two measurement schemes were considered. One required that the bubble be stationary when the field of view is scanned by the camera. Two measurements would be made; one before the application of the drive field providing the initial bubble position; the second after the displaced bubble motion has been arrested. Inherent in this technique is a small amount of postion error caused by overshoot.

The second scheme required that the second measurement be taken during the drive field "on" cycle. Because of the slow scan rate of the video camera (16,666 microseconds/ frame) additional circuitry would be required to sync the drive field pulse application to the scan line's approach to a bubble so as to overtake the bubble during the period of motion. In addition to the extra circuitry involved and the increase in design complexity, the amount of data obtained per scan would be less than that obtained using the stationary technique. An optical/photographic technique for obtaining dynamic mobility measurements has been suggested by Humphrey at the California Institute of Technology (Ref 1:202-208).

Because of the lesser design complexity and amenability to total automatic implementation, a stationary mobility measurement design was chosen. Figure 1 presents a functional block diagram of the bubble measurement system. A quality microscope is required in the system for two reasons. The size of the bubbles in material currently under development is two micrometers making high magnification necessary. Because of the small bubble size and the sensitivity of

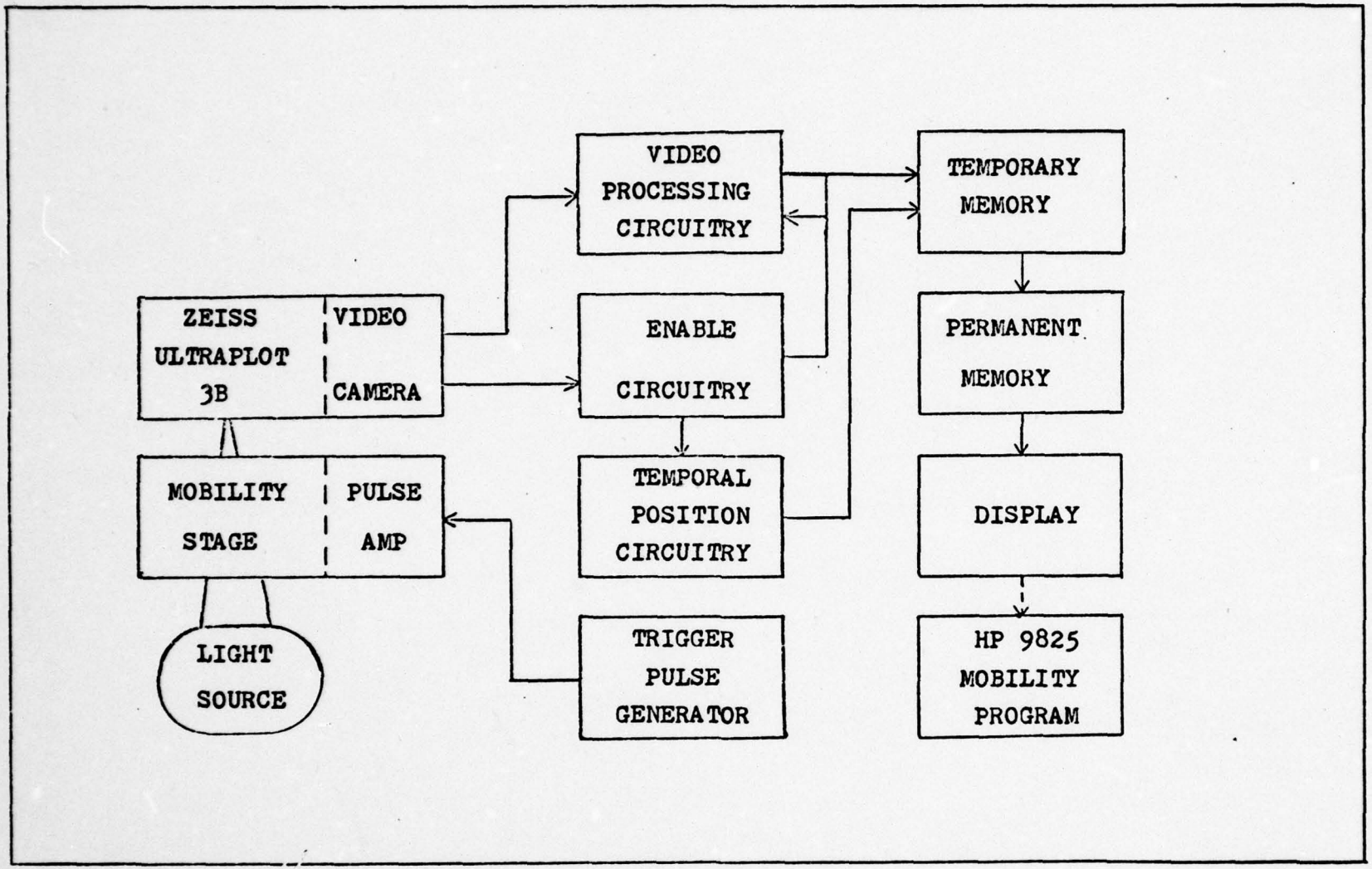

Figure 1. Functional Block Diagram of Mobility Measurement System.

plumbicons, high grade optics are a must for maximum light transmission. The above system employes a Zeiss microscope.

The mobility stage provides two very important functions. A large solenoid mounted on the stage provides the magnetic bias field perpendicular to the anisotropy plane required to coalesce the domain stripes into cylinders. A gold conduction pattern deposited on a microscope slide is used to generate the "in-plane" magnetic field gradient necessary to drive the bubbles.

Figure 2 displays the major features of the mobility stage. Chapter 3 contains a detailed description of the bubble mobility stage.

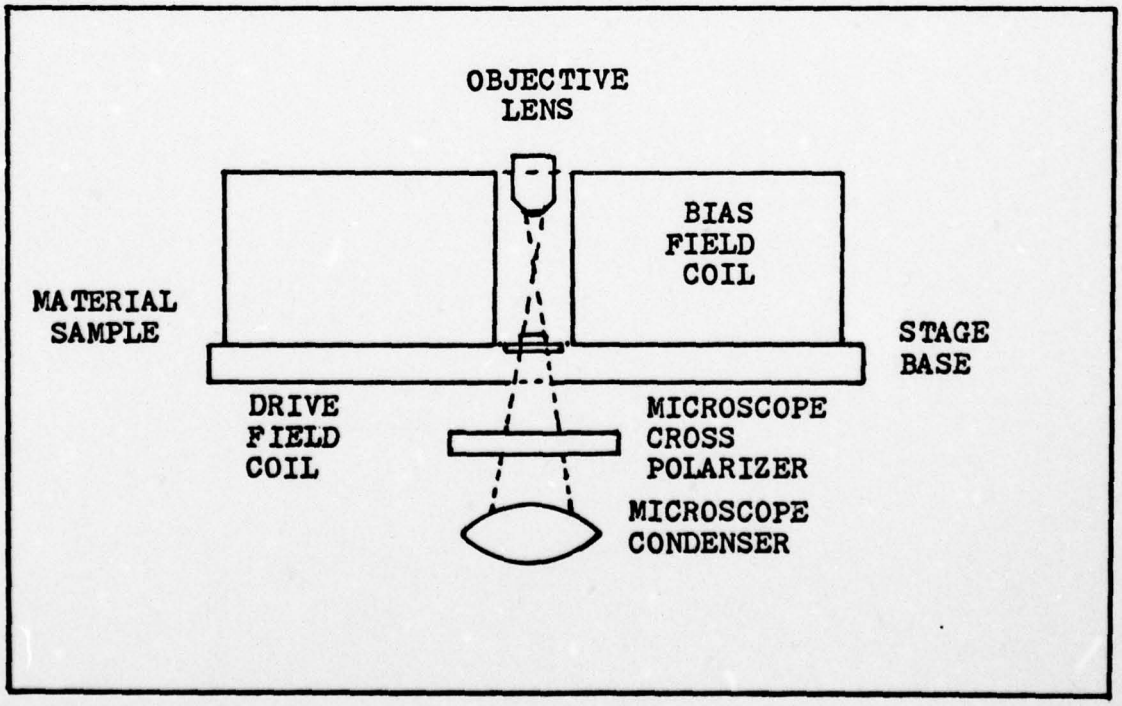

Figure 2. Basic Make-Up of the Bubble Mobility Stage.

A Telemation TMC 1100 television camera was used in the role of light-to-voltage transducer. The plumbicon-equipped camera has two important features. They are a one volt peak-to-peak output at 0.01 lumen illumination and a variable black level. Use of an 800 line camera yields 400 line/frame resolution. Only one field was used to extract the bubble position data eliminating the problem of two-field scan and associated time ambiguities. Circuitry involved in this process is located on the video processing board.

The video processing board is one of the three sections of the electronics package. Figure 3 is a block diagram showing the subsystems of the electronics package.

The video processing board contains most of the circuitry involved in bubble discrimination and time position generation. It is functionally divided into five sections. The video discrimination/level detection section extracts the domain signal from the video contrast signal. The level detection circuit yields an output for voltage levels greater than the camera black level. Output from the level detector is processed by the bubble time filter to decrease the amount of data collected per bubble.

The data enable circuitry insures that data is taken only during on field scan. This is accomplished by enabling the temporal position generator and the memory enable circuitry only during one vertical scan period. The temporal position generator provides the time analog of the

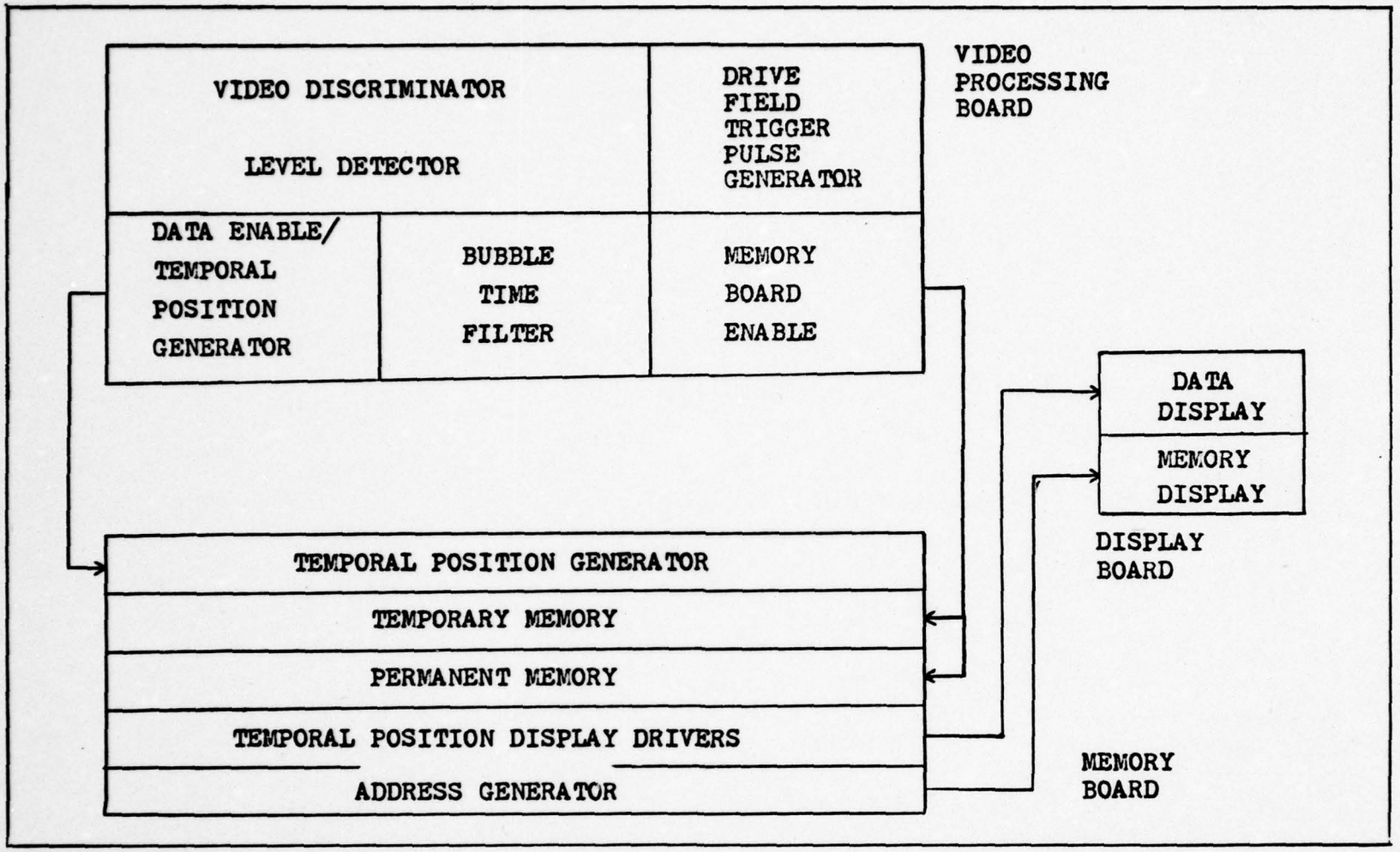

Figure 3. Functional Block Diagram of Electronics Package.

bubble's spatial position. Pulses from the memory board enable circuitry load the temporal position data into temporary and permanent memories respectively. A 20 bit word is used because counting is done in base ten. A 16 bit word would be sufficient when using base sixteen. Data is extracted from the memory using the temporal position display. The drive field trigger pulse generator provides a single 30 nanosecond pulse to the E-H model 123 pulse generator used to generate the drive field. Detailed circuit and operating descriptions of the electronics package are contained in Chapter 4.

Due to late delivery of a Hewlett-Packard (HP) 9825 minicomputer, no interfacing was designed. The 9825 was used to compute the bubble mobility from data stored in the R/W permenent memory. Chapter 5 contains a detailed description of the mobility calculation program.

III. Bubble Mobility Stage

One system segment common to all the system designs considered is the mobility stage. The purpose of the stage is to provide the magnetic bias field and the in-plane drive field required for mobility measurement work. Three stages were designed. The initial design was based on constraints imposed by the material and by the available equipment. The subsequent designs resulted primarily from convenience considerations.

Initial Mobility Stage Design

Early in the program, a Leitz student microscope provided the means for observing the domains. The author decided to construct an attachable stage using the microscope stage as a foundation. Because of the decision to "piggyback", the primary limitations on the mobility stage's physical dimensions were the microscope construction and optics.

The maximum thickness of the stage (top of the

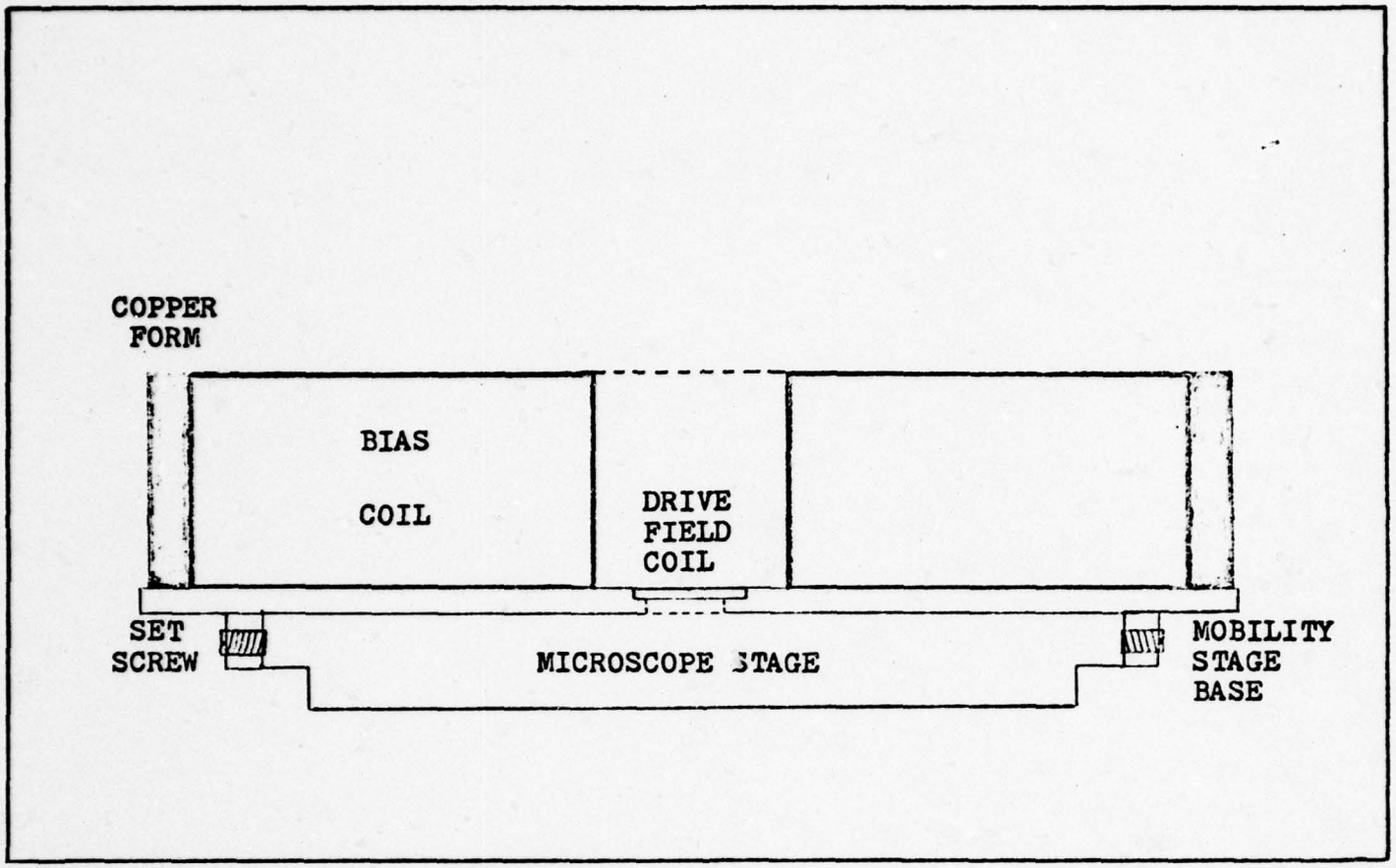

Figure 4. Elevation View of Initial Mobility Stage Design.

microscope stage to the top of the garnet sample) was limited to less than 3.5 millimeters due to the focal length of the condenser lens. The use of high power objective lenses resulted in vety short focal distances which limited the maximum bias field coil height to 30 millimeters. The microscope cradle limited the maximum stage base diameter to 153 millimeters. Figure 4 displays an elevation view of the initial mobility stage design.

Although a maximum of 153 millimeters was available for the coil and stage diameters, the coil was made 120 millimeters in diameter to provide room for attachment mechanisms.

Because of the strict tolerances required by the condenser lens focal length, this design was not considered usable. The stage base thickness was limited to less than 3.5 millimeters which was not considered sufficient. A new stage design based on the total replacement of the microscope stage by the mobility stage was conceived.

Mobility Stage- Mod 1

Figures 5 and 6 show top and elevation views of the modified mobility stage respectively.

The modified stage base consists of a round, 8mm thick, 140mm O.D. aluminum plate. The three 4mm holes drilled in the base provided the means of attaching the stage to the

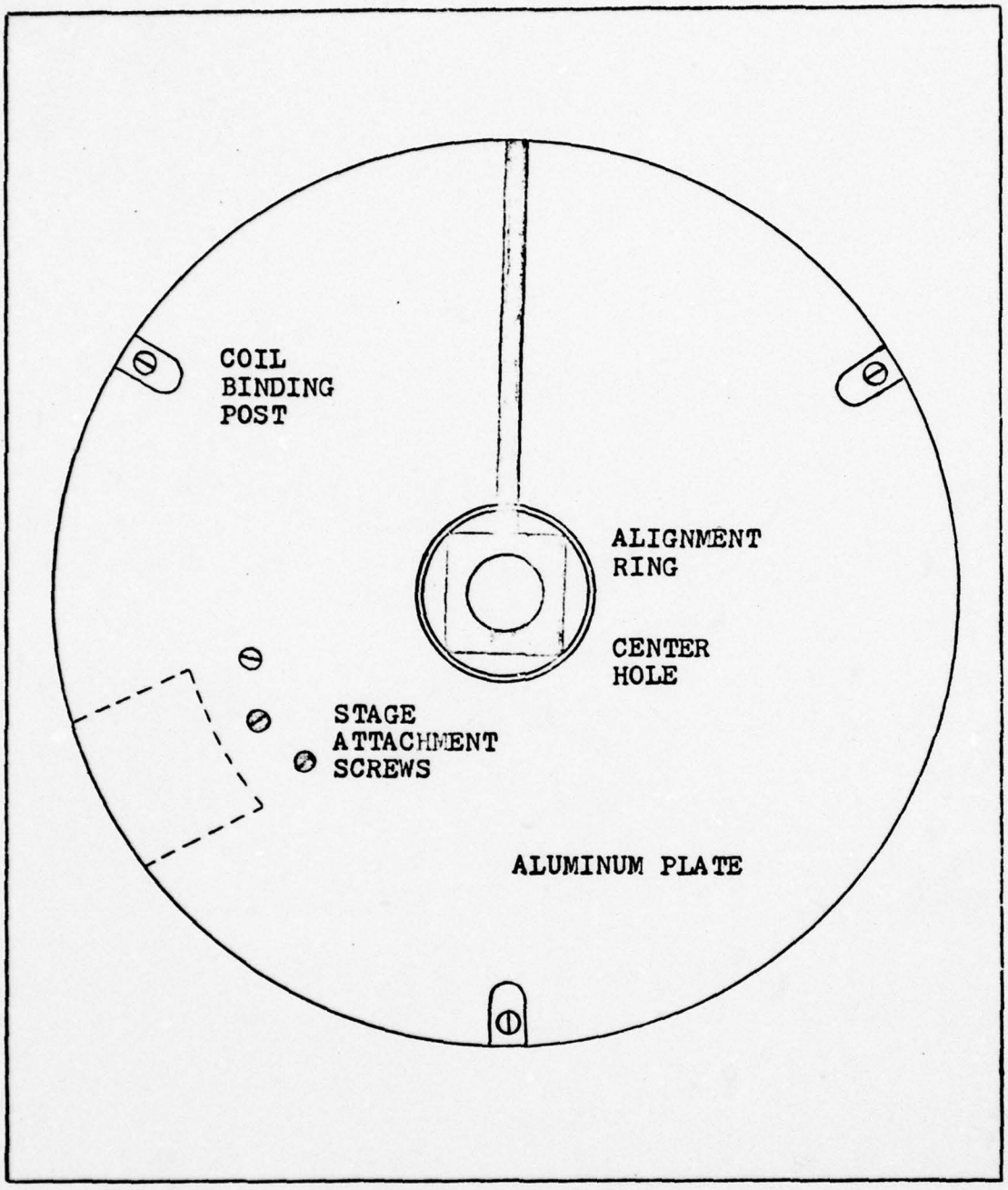

Figure 5. Top View of Modified Mobility Stage.

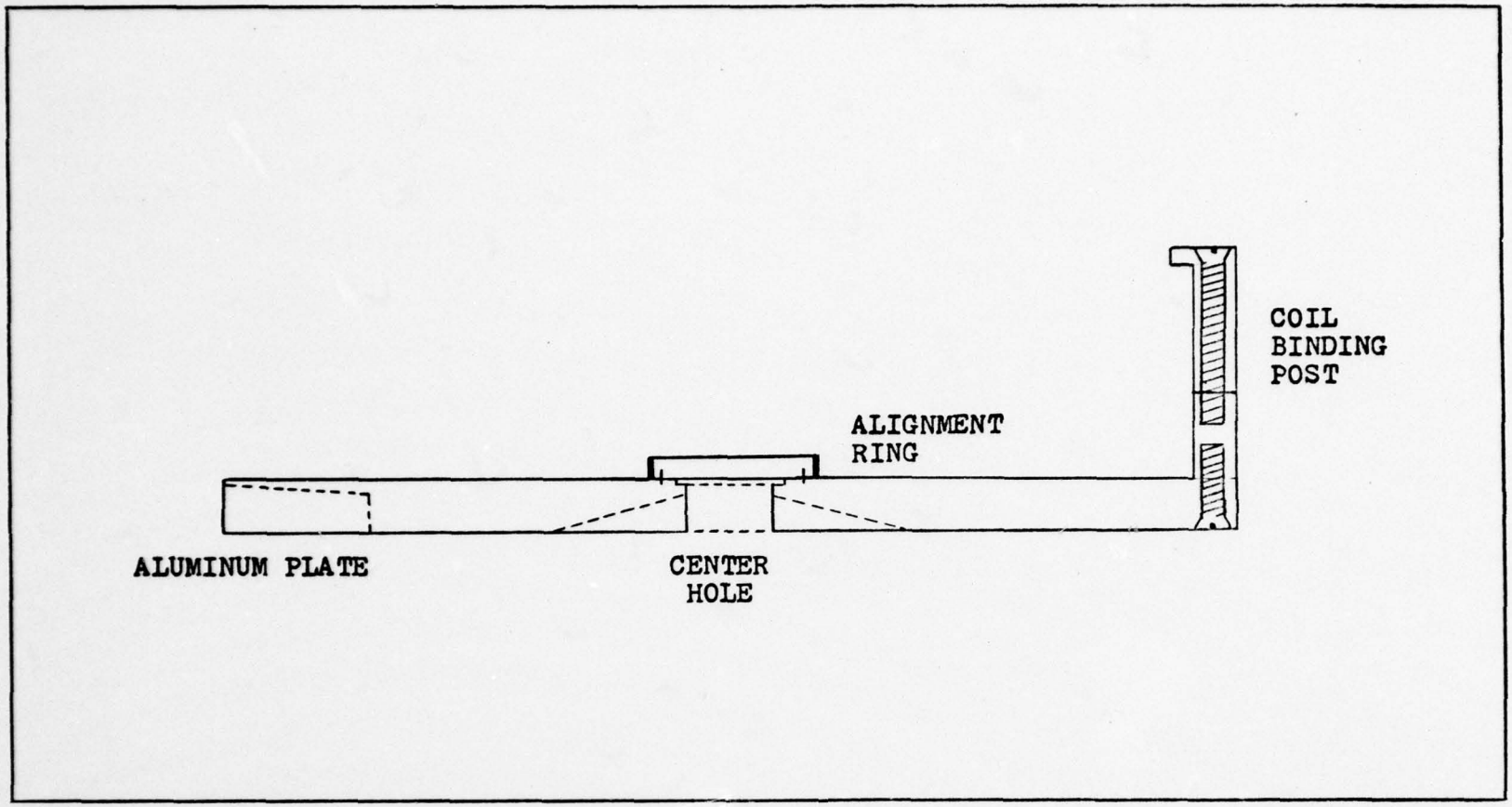

Figure 6. Elevation View of Modified Mobility Stage.

microscope. A 12.7mm center hole bored in the base allows for sample transmission illumination. Three 34mm x 6mm tapped posts are used to attach the bias coil to the base. By loosening the binding post screws, the coil easily detaches from the base making sample changing easier than for the initial design. The 3mm x 23.4mm center sleeve assures alignment between the coil and the sample area. The drive field coil consists of a thick film gold metallization pattern deposited on a 1mm thick, 22mm square glass slide. Through mounting the drive field slide in the base and milling the bottom of the base to permit maximum extension of the condenser lens, the condenser lens focal length criterion was met. A 25.4mm x 25.4mm notch milled from the base underside was necessary for microscope frame accommodation.

The coil design was modified slightly. In lieu of the copper frame used for heat dissipation, a brass frame was used. The 25.4mm I.D., 139.7mm O.D., and 30mm high dimensions remained unchanged. Eleven hundred and sixty turns of #18 Belden magnetic wire were wound around the frame. Using a 40 VDC, 20 amp power supply, a variable magnetic field strength (gauss) controlled by the applied voltage (VDC) on the coil was obtained. Figure 7 presents the H versus VDC curve for the mobility stage bias coil. Using the values of voltage and current at each measurement point, a mean coil resistance of 6.4 ohms was calculated.

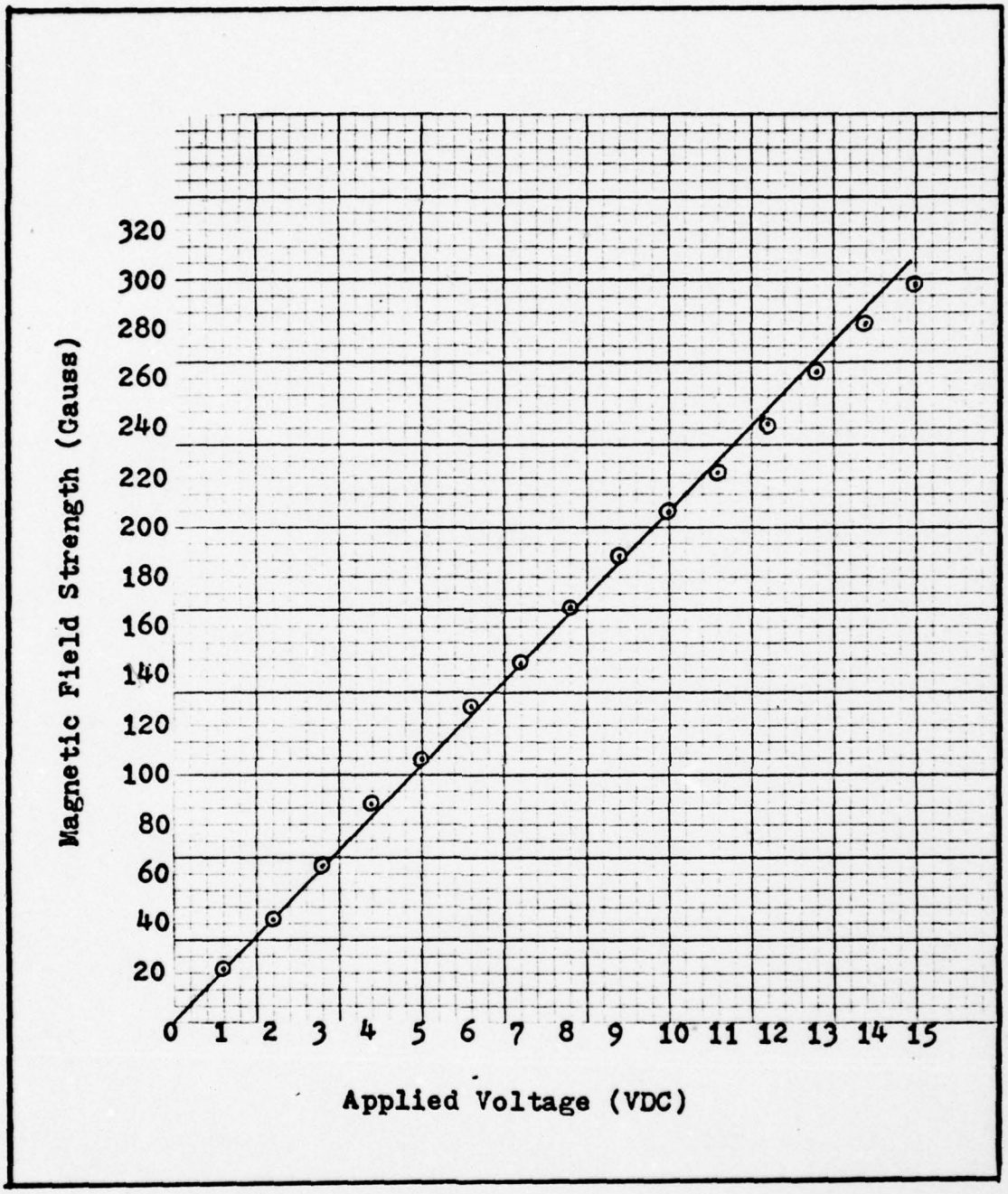

Figure 7. Bias Field Coil H versus VDC Curve.

A new Zeiss ULTRAPLOT 3B microscope arrived shortly after completion of the modified mobility stage/bias coil, making the Leitz student microscope obselete. The Zeiss has a 165mm diameter stage and a condenser system with a focal distance in excess of 9mm. The mobility stage/mod 1 would have been adquate except that the microscope's lowest stage stop did not provide enough clearance for the mobility stage to ride piggyback. In order to place the mobility stage on the microscope stage, the microscope stage had to be removed, the mobility stage set in place, and the microscope stage replaced. Each sample change would have required the above proceedure. To alleviate this problem, additional modifications to the mobility stage were required.

Final Stage Design

The only change in the mobility stage/mod 1 design involved the sample changing problem. A dovetailled drive field coil/sample holder was designed. Figure 8 shows top and elevation views of the stage base. Figure 9 shows top and elevation views of the sample holder.

As before, the base consists of a 140mm O.D. aluminum disk, 8mm in thickness. Three 30mm binding posts provide the means for attaching the bias coil. A 50.8mm wide x 6.3mm deep x 124.5mm long area was milled from the

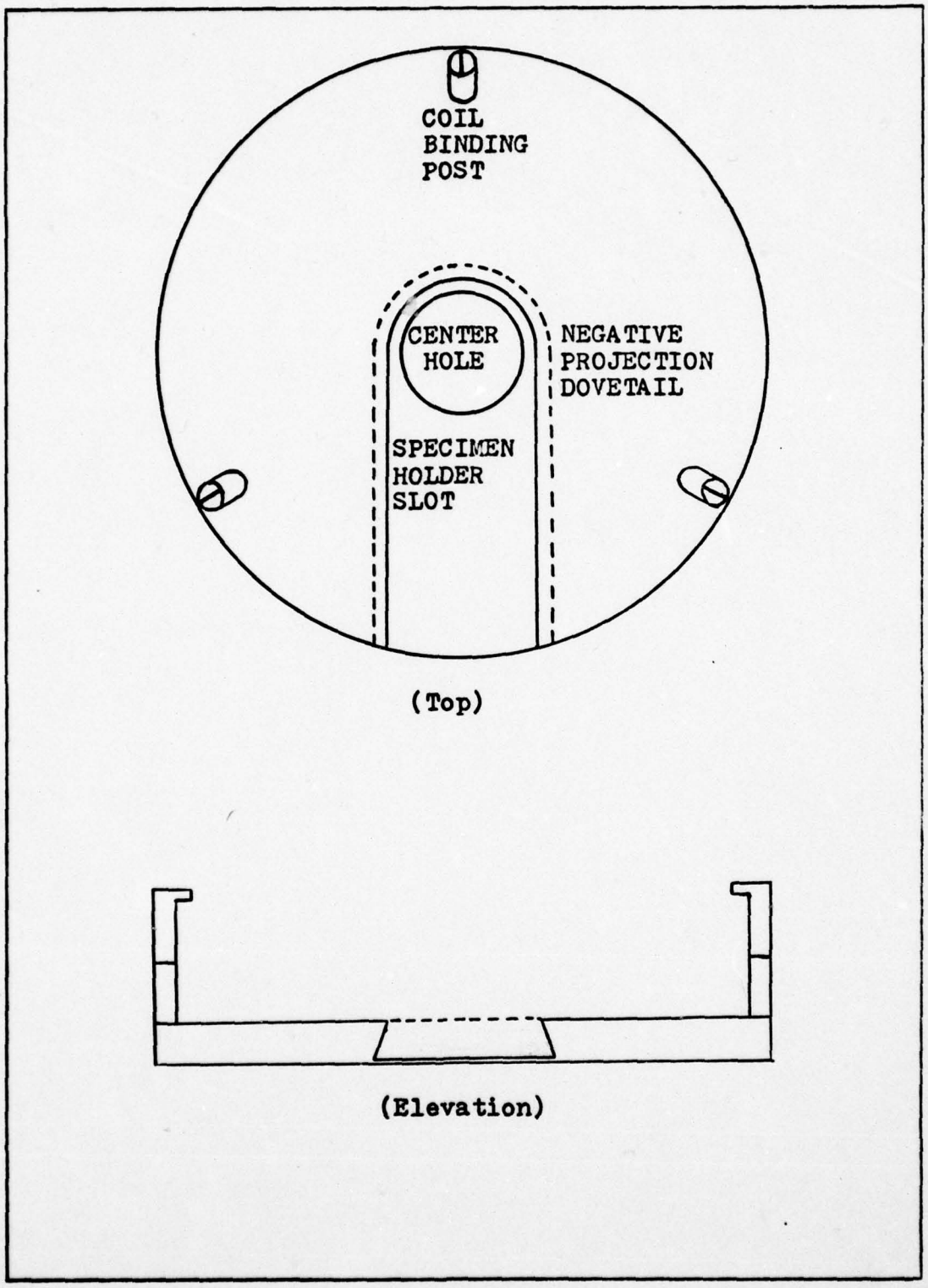

Figure 8. Top and Elevation Views of Final Stage Base.

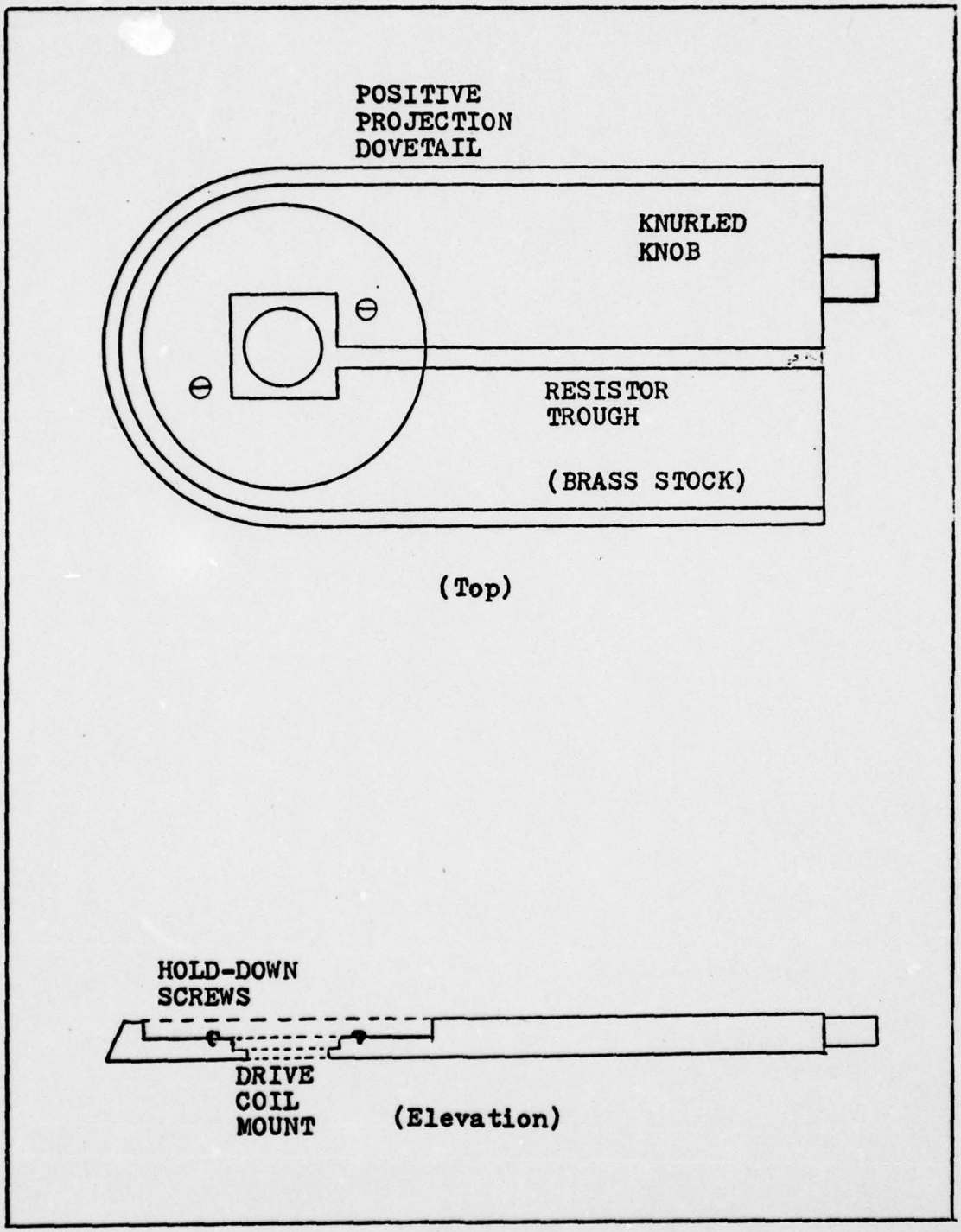

Figure 9. Top and Elevation Views of Brass Sample Holder.

base top to provide space for the sample holder. A 3.2mm dovetail (negative projection) was milled from the perimeter to act as the holder guide and lock. A 12.7mm hole drilled in the base center allows for illumination transmission.

Two specimen holders were constructed from brass. The outside dimensions are approximately those given for the milled area in the stage base. An area 44.4mm in diameter centered over the base center hole was milled to a depth of 4.1mm. A centered square area 16mm on a side was milled an additional depth of 1.3mm in order to hold the drive field coil slide. The center 12.7mm of the circular area was drilled through to allow for illumination transmission. Two brass clips are used to hold the sample/drive field coil slide in place. The specimen holder has a 3.2mm positive dovetail projection around its perimeter. A 5.8mm wide x 4.8mm deep x 76.2mm long trough milled from the left center (from the coil area to the exposed end) of the holder permitted the wires and 50 ohm load resistance to be mounted on the specimen holder instead of externally. A 9.5mm knurled knob on the exposed end aids in handling the holder when installed in the base.

The only external connections to the base and holder are the bias supply connections and the drive field coil supply connections. A 0-40 VDC, 20 amp power supply provides a bias coil supply source. An E & H model 123 pulse generator capable of 1 ampere output into a 50 ohm load for as short as 20 nanoseconds fulfills the drive field coil power

supply requirement.

The 123 does not have a single pulse mode. This is compensated for using a 30 nanosecond monostable multivibrator trigger pulse generator located on the video processing board as the external trigger. The following chapter contains a complete description of the mobility stage's electronics.

IV. System and Electronics

In order to exploit the use of a computer in the mobility measurement scheme, it is necessary to extract the bubble position from the video contrast signal and place this information in computer compatible form. The purpose of the system's electronics is to accomplish this task. The following text describes the video processing, timing, and memory circuits and their function. Also described are the chassis and board IC layouts.

Video Processing Board

The video processing board can be divided into five functional areas as shown in Figure 3 of Chapter 1. Video contrast information is fed from the video camera to the video discrimination/level detection section input. Figure 10 shows a schematic of this section. An Lm 741CN is used in conjunction with a Motorola SK3066 reference zener diode to form a precision positive reference voltage source. The output of this circuit can be varied from 0.15 to 12.6 volts

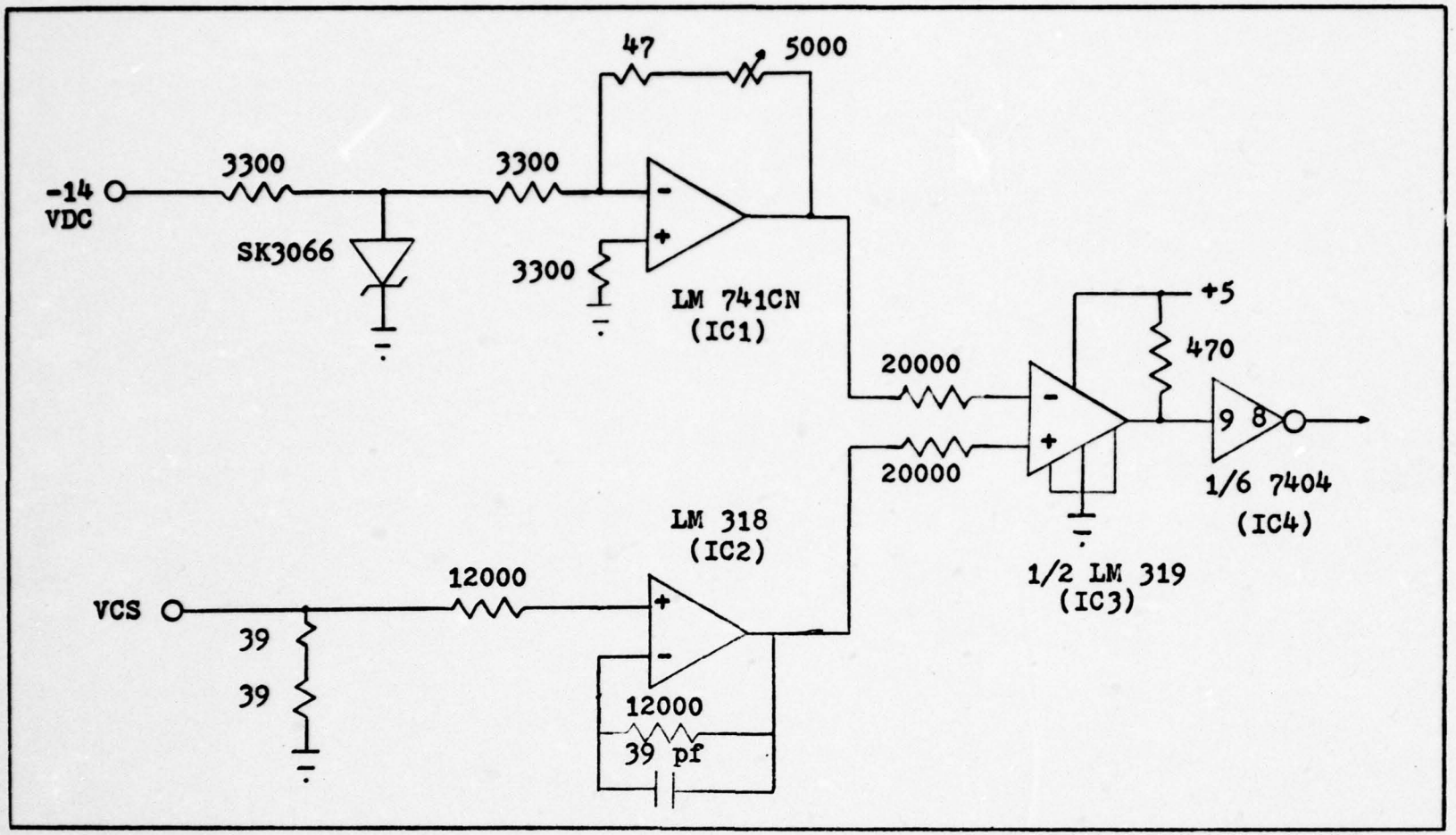

Figure 10. Schematic of Video Discriminator/Level Detection Circuit.

byvarying the 5000 ohm potentiometer in the feedback loop. An LM 318 (IC2) provides the basis for a non-inverting 3.7 MHz low pass filter which attenuates any higher frequency noise in the video contrast signal. IC3 is an LM 319 dual precision high speed voltage comparator.

The outputs of IC1 and IC2 are fed to the number one inputs (pins 4 and 5) of IC3. The reference voltage is adjusted until only the presence of a bubble yields an output. This acts as an additional noise filter. Through the use of a pull-up resistor, a TTL compatible output results at IC3 pin 12 when the video contrast level exceeds the reference voltage level. An inverter from IC4 (7404 hex inverter) inverts the comparator logic making it comparable with the 74LS124 (IC10) enable logic.

Figure 11 shows a schematic for the bubble time filter. IC10 is a dual voltage controlled oscillator chip. The 'LS124 has a guaranteed frequency spectrum on 1 to 20 MHz with typical power dissipation of 150mW. A 50 percent duty cycle is provided.

A 5 MHz operating frequency is achieved using a series combination of a 10pf ceramic capacitor and a 5 MHz crystal across pins 4 and 5. The enable, gating, and output sections' supply voltage are +5 VDC. The oscillator and frequency control circuitry supply voltage is lowered to approximately +3 VDC through the use of a simple voltage divider network involving a 220 and 330 ohm resistor. The range and frequency control inputs are grounded for maximum

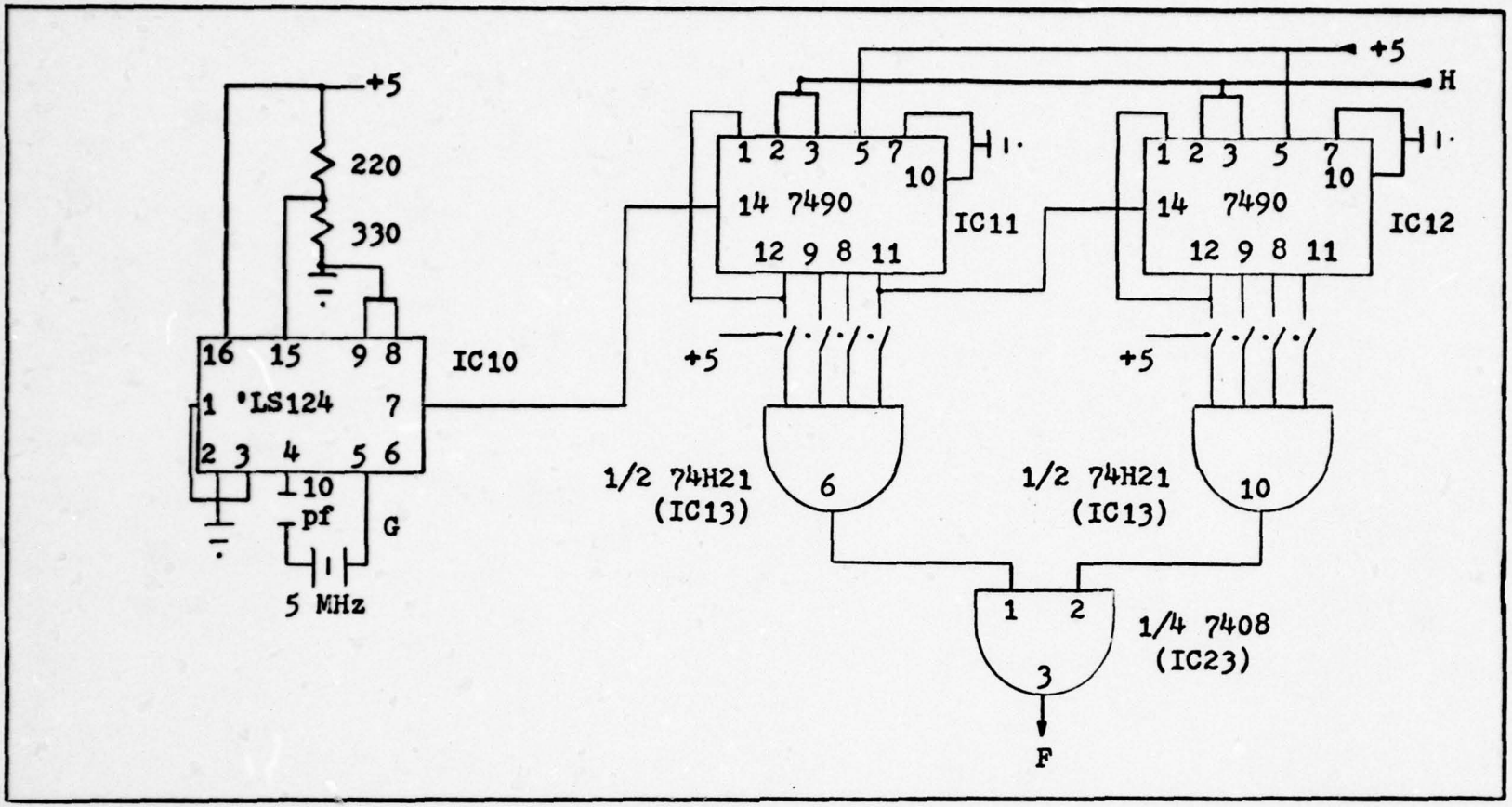

Figure 11. Schematic of the Bubble Time Filter Section.

stability. Two 7490 decade counters (ICs 11 and 12) are used as a discriminator. Their outputs (pins 12, 9, 8, 11) are connected to one of the posts of 8 SPDT minature slide switches. Supply voltage is connected to the other switch posts. The switch common posts are connected to the inputs of a 74H21 (IC13) dual 4-input AND gate chip. The outputs of IC13 (pins 6 and 8) are fed to pins 1 and 2 of IC23, a quad 2-input AND gate chip.

A 5 MHz operating frequency was chosen in order to provide a 200ns time resolution capability. This choice was based on the premise that camera line scan times would be between 25 and 53 microseconds, and that microscope powers in excess of 1000x would be used. Thus a domain covering 5 percent of the microscope field of view (FOV) at its (the domain) maximum width would ideally yield a maximum of 13 time pulses.

The 8 SPDT switches can be set to accept either the output of ICs 11 and 12, +5 VDC, or a combination of the two. The time during which the output of IC3 (level detector) is required to be high (VCS above the camera black level) is set using the combination of switches in the 7490 position. All unused switches are set to the switch/+5 VDC position. To detect a count of 13, the switches for IC11 would be set as follows: pins 9 and 12 to the 7490 output position and pins 8 and 11 to the +5 VDC position, while the switches for IC12 would be set as follows: pins 11, 9, and 8 to the +5 VDC position and pin 12 to the 7490 position. If the

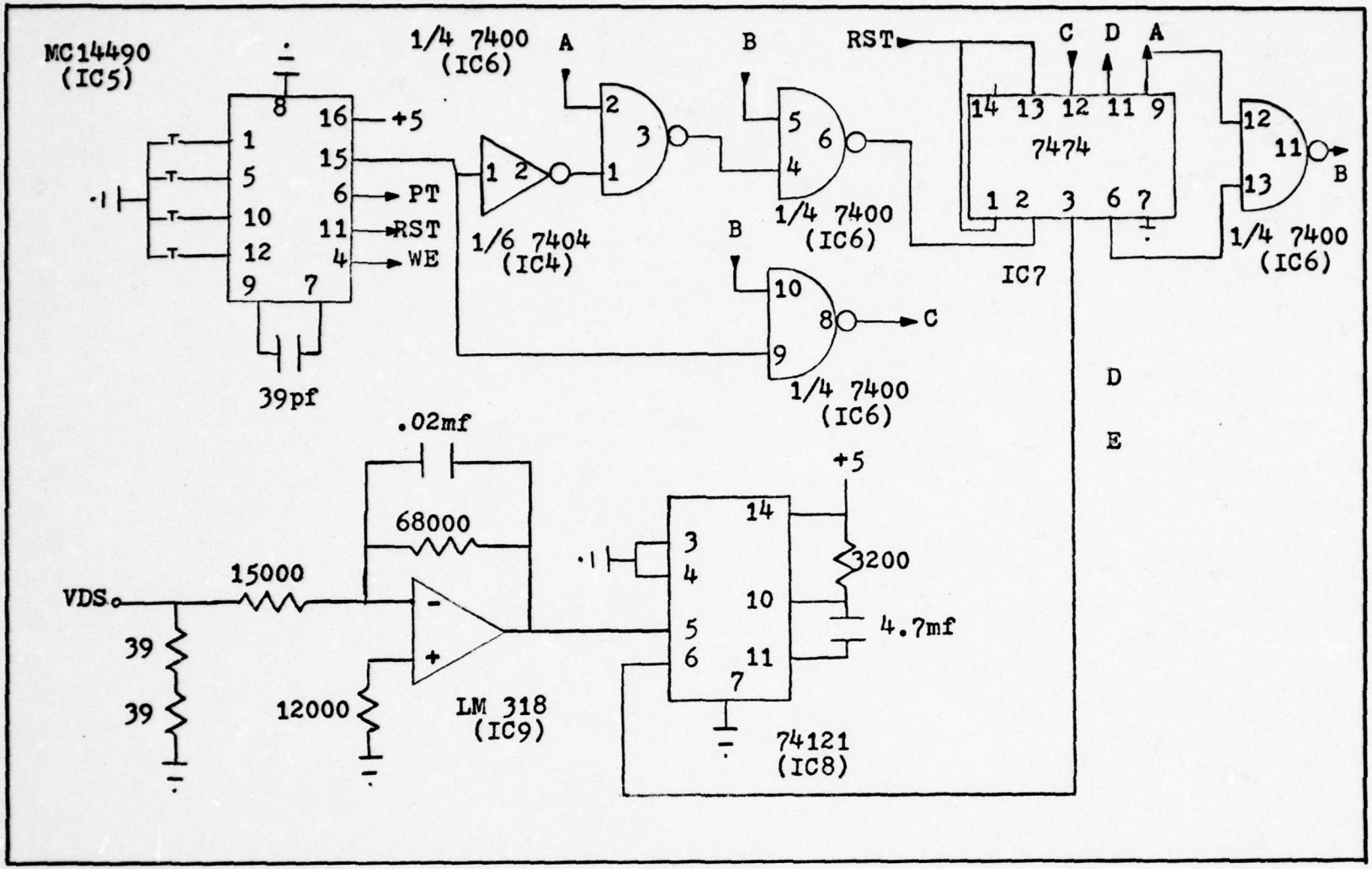

Figure 12. Schematic of Data Enable Circuit.

level detector output remains "high" for at least the time set by the switch positions, the outputs of IC13 go high, causing the state of pin 3 (F), IC23 to go "high" for 100 nanoseconds (50 percent duty cycle). Signal F is fed to pin 9 of IC23 establishing half the required signals necessary to activate the memory enable circuitry.

The other input signal (E) to the memory board enable circuitry is generated by the data enable circuitry. Figure 12 shows a schematic of the data enable circuitry. IC5 is a MC14490 hex contact bounce eliminator which provides the external, debounced signals required in the electronics package. The DATA ENABLE (DE) signal is generated on the package front panel (to be described later) using a momentary contact SPST switch. This switch provides the input to IC5 pin 1. When the switch contact closes, the state of IC5 pin 15 goes "low", providing one of the two required enabling signals in the circuit. The second enabling signal is generated by the vertical drive signal (VDS) processing circuitry.

Figure 13 presents the overall timing diagram for the data enable circuit.

As can be seen from Figure 13, the output of IC6 pin 11 is initially "high", disabling the time position generator. If the DE button is not depressed, the initial conditions established on IC7 do not change the status of pins 9 and 7 (IC7) when the state of pin 6 IC8 is "high". Enabling the circuit (DE depressed) alters the state of

IC6 pin 8. The next vertical drive pulse (VDS) causes the state of IC6 pin 11 to go "low", enabling the position generator.

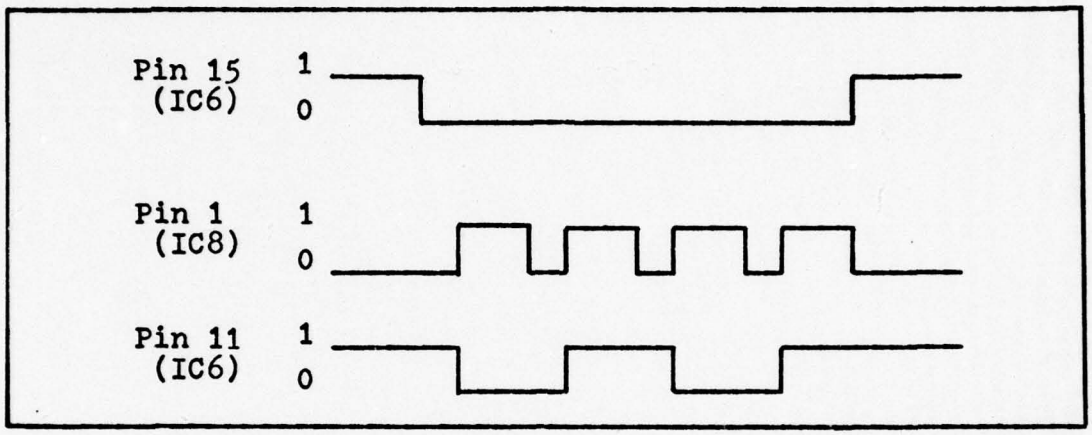

Figure 13. Overall Timing Diagram for Data Enable Circuit.

While the DE switch is depressed, every third vertical drive pulse causes the circuit to process the incoming VCS data. After the DE button is released, the last domain position data processed remains in the memory. The output of IC8 pin 1 (CR) is used to reset the time position counters and the memory address generator (IC35).

IC14 (74LS124) is enabled when the state of IC6 pin 11 goes "low". IC14 is constructed identically to IC10 except that a 1 MHz crystal is used to generate a 1 MHz frequency. Figure 14 shows a schematic of the temporal position generating circuitry. The output of IC14 pin 7 is fed to five serially connected 7490 decade counters

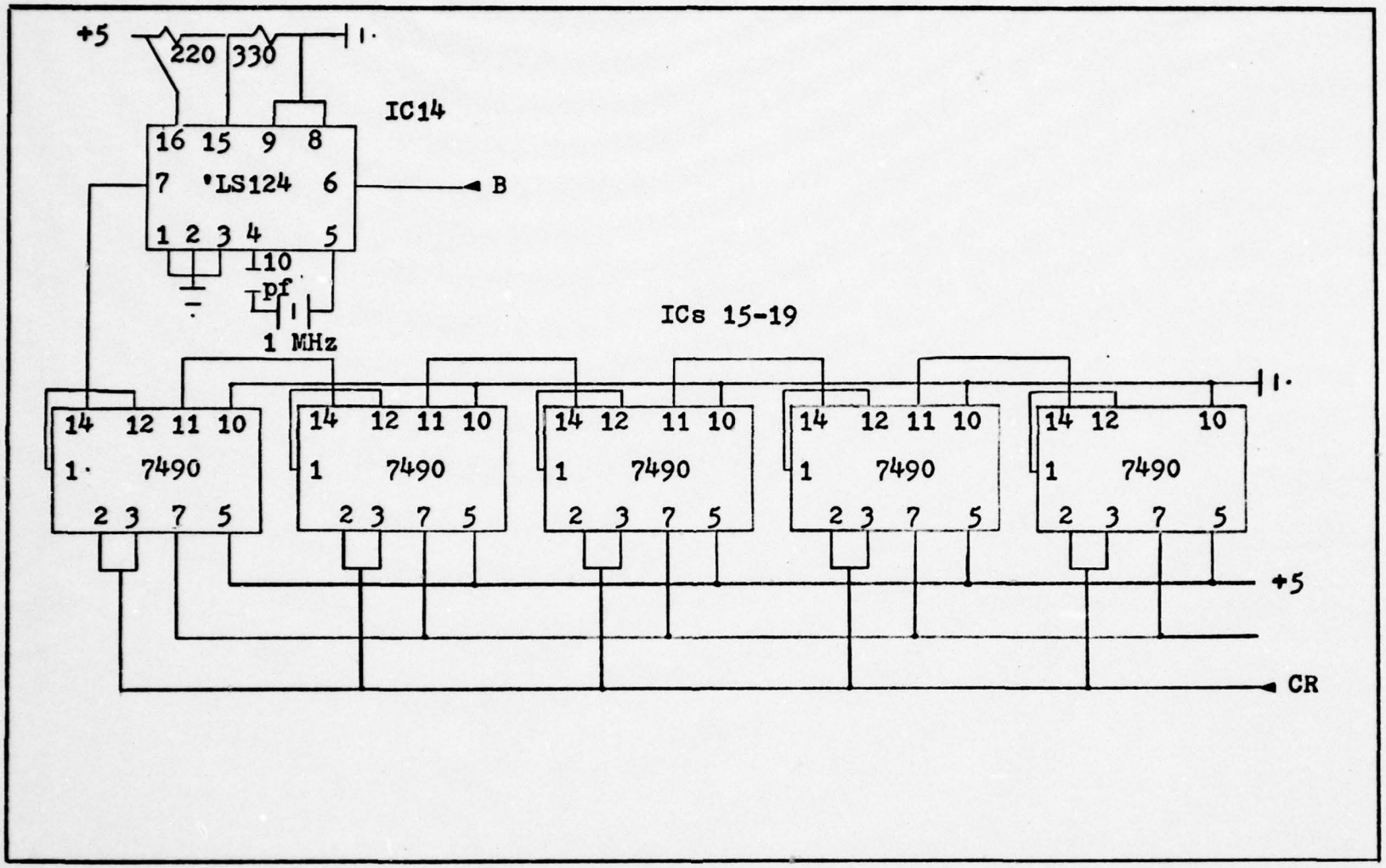

Figure 14. Schematic of Temporal Position Generating Circuit.

(ICs 15 through 19). The serial counters yield a maximum count of 99,999 of which only 16,666 is used (time in microseconds equal to one camera frame). ICs 15 through 19 are located on the memory board and their output feed into the temporary memories.

Signals E from the data enable section (16,000 microsecond duty cycle pulse from the monostable multivibrator, IC8) and F from the bubble time filter section are fed to IC23 using pins 9 and 10 (see Figure 15). The state of IC23 pin 8 going "high" indicates the criteria for a domain has been met and the data enable circuit is indicating a scan frame. IC20 is designed as a 100ns duration positive edge triggered monostable multivibrator. The state of IC23 pin 8 going "high" triggers the monostable clocking the temporary memories and storing the count from ICs 15 through 19.(the time equivalent of the domain's spatial position in the microscope FOV). The state of IC20 pin 6 is fed to IC21 pins 3 and 4. IC 21 is designed as a negative edge triggered monostable with a 100ns pulse duration. The state of IC21 is NORed with the READ/WRITE SWITCH output (on front panel). IC42 pin 3 (7402 quad 2-input NOR gate) is connected to lug 3 on the video board. IC5 pin 4 provides the WRITE ENABLE (WE) pulse to lug 2 on the video board. The ME and WE signals (PM ENABLE) enable the permanent memories on the memory board. The state of IC21 pin 6 is also fed to pins 3 and 4 of IC22. IC22 is designed as a negative edge triggered 30ns pulse

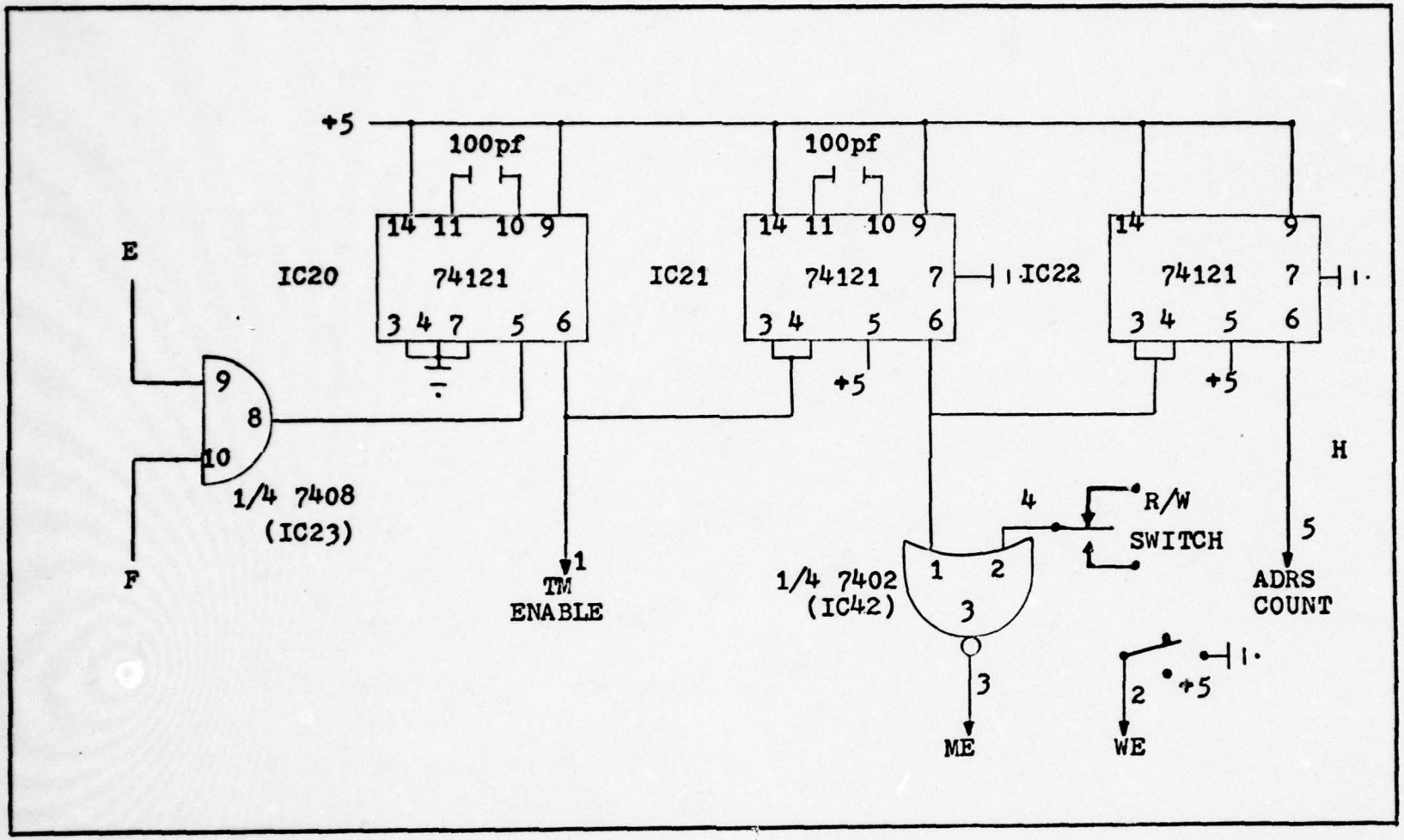

Figure 15. Schematic of Memory Board Enable Pulse Generators.

duration monostable which provides the memory address update pulse to IC35. Figure 16 shows the memory enable pulse generating circuitry timing diagram. The state of

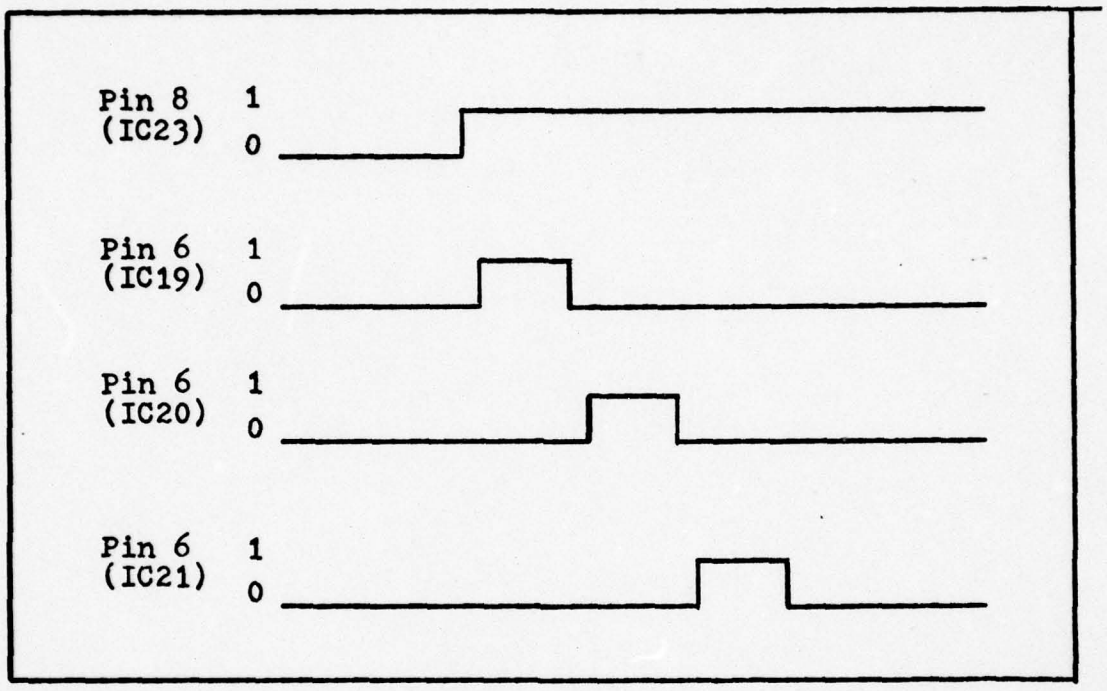

Figure 16. Timing Diagram for Memory Enable Circuitry.

IC22 pin 6 (H) resets the time filter counters after each update of the address location.

IC5 pin 6 provides the input pulse to the external 30ns trigger pulse generator required to enable the E&H Research Laboratories Model 123 pulse generator/amplifier. A 50 volt peak-to-peak output pulse of 1 to 2 microseconds duration from the 123 is fed to a parallel combination of 1/4 watt, 100 ohm resistors (50 ohm load requirement). Pads 1 and 4 of the drive field metallization pattern (see Figure

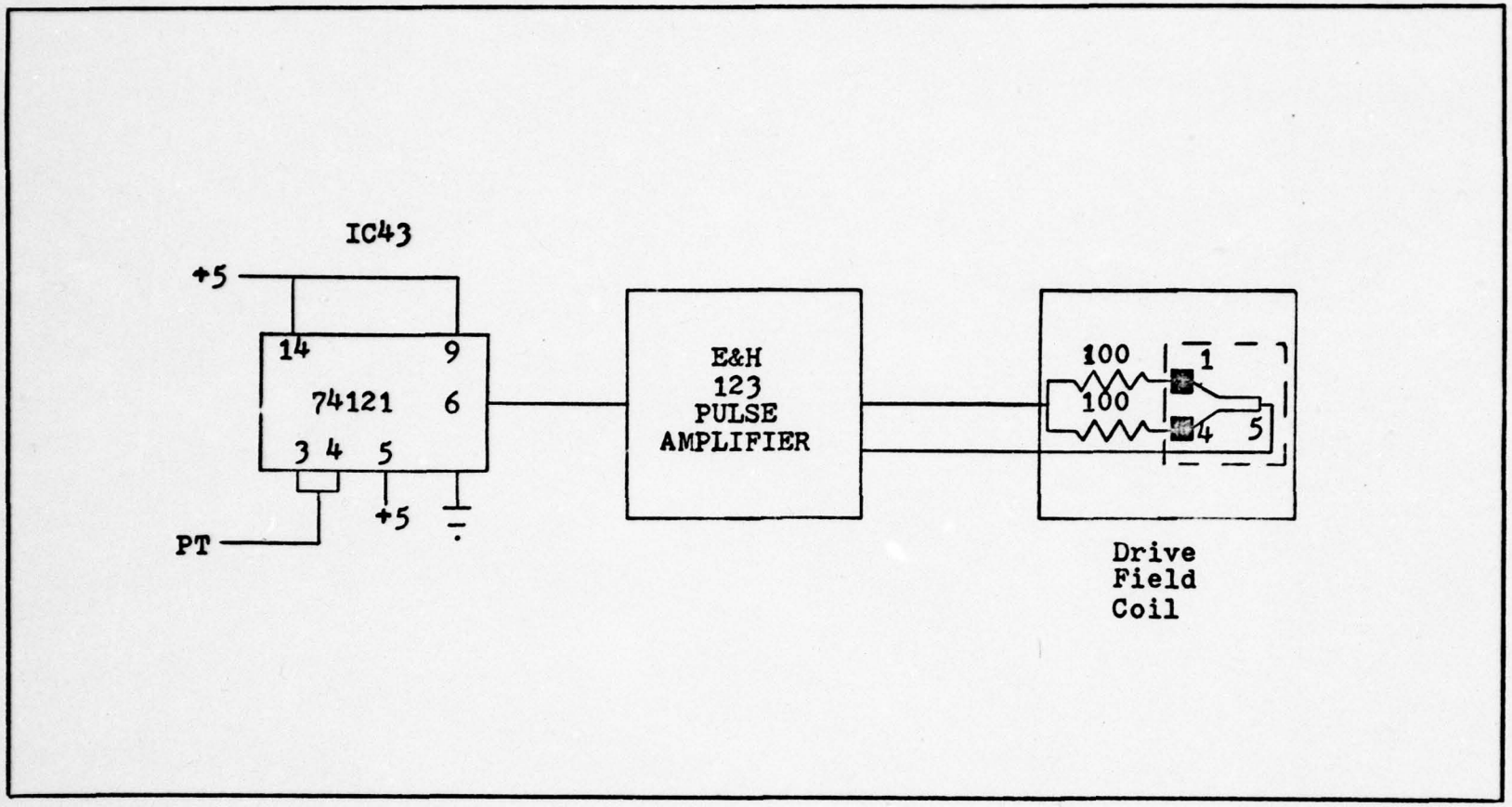

Figure 17. Schematic of Mobility Stage Electronics.

17) are connected to the 100 ohm resistors. Thus the 0.5 amperes feeding each pad generates a magnetic field gradient within the bias field. The ground connection is made at pad 5 of the metallization pattern.

Figure 18 provides a diagram of the major signal paths in the electronics board circuitry.

The video processing board is the electronics package central control unit. All the storage and information retrival circuitry is located on the memory and display boards.

Memory Board

Figure 19 shows the schematic for the temporary and permanent memory circuitry. ICs 24 and 25 are 74100 8-bit bistable latches. IC26 is a 4-bit bistable latch. The outputs from ICs 15 and 16 are fed to IC24. The outputs from ICs 17 and 18 are fed to IC25. Data from IC19 are fed to IC26. Data from the 7490 decade counters are transferred to the Q output of the latches (IC 24 and 25) when the TM ENABLE state goes "high". ICs 27, 28, and 29 are 7404 hex inverter chips. ICs 30 through 34 are 7489 64 bit read/write memories. The complements of the data written into memory are non-destructively read out. Because of the complement operation of the memory ICs, ICs 27, 28, and 29 are used to invert the logic at the Q outputs of ICs 24 and 25. IC26

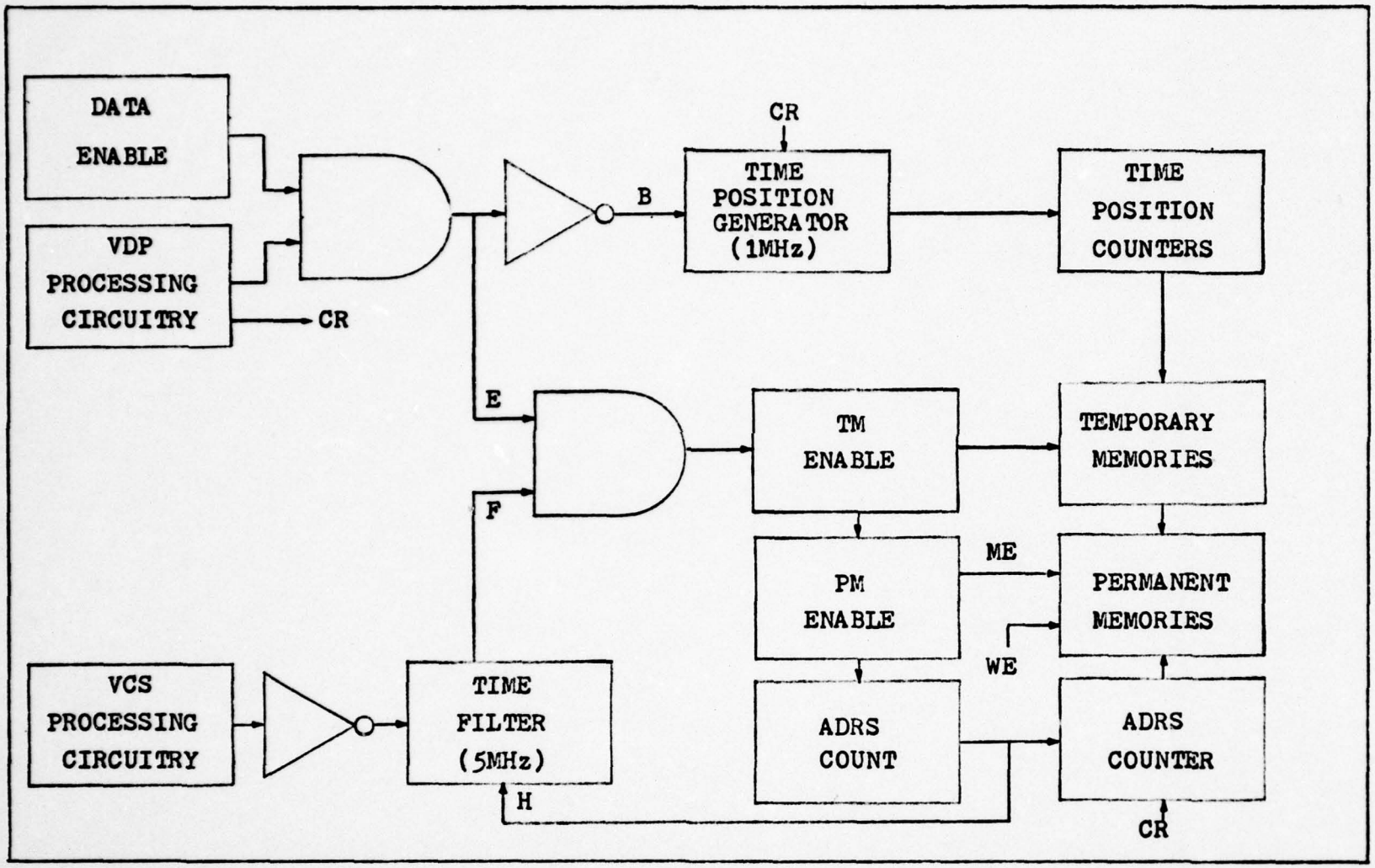

Figure 18. Functional Block Diagram with Signal Paths for Electronics Package.

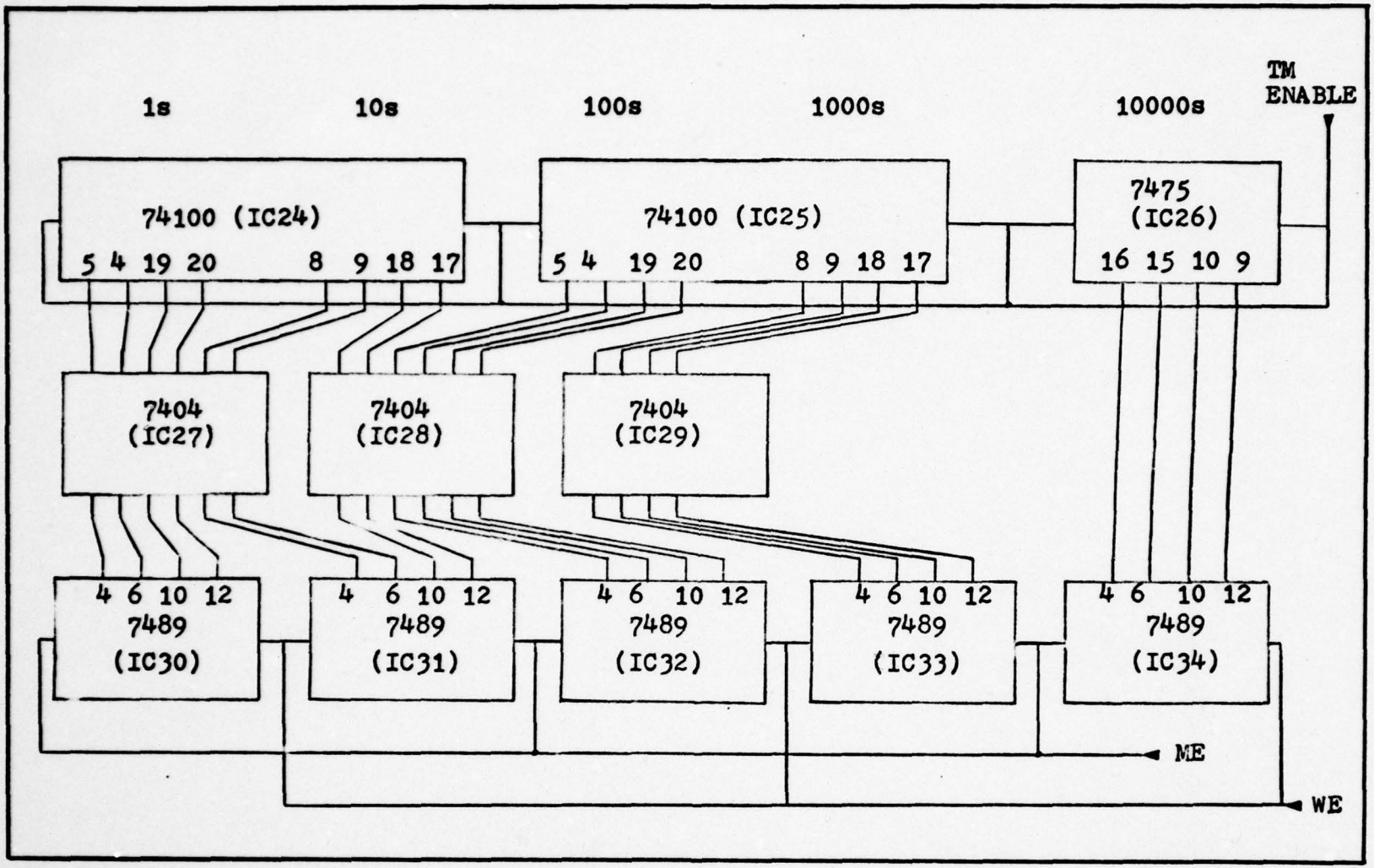

Figure 19. Schematic of Temporary and Permanent Memory Circuitry.

has $\bar{Q}$ available on the chip. Approximately 40ns after the TM ENABLE state goes "high", the complement of the temorary memories' Q state are available at the 7489 data inputs. The PM ENABLE state goes "low" approximately 100ns after the TM ENABLE change of state. With the PM ENABLE "low", the data are written into memory. Approximately 100ns after the data are written into memory, the ADRS COUNT pulse advances the address position by 1 and resets the bubble time filter counters.

Figure 20 shows the schematic for the address count and display circuit. IC35 is a 7493 4-bit binary counter. Signal CR from IC8 pin 1 resets IC35 whenever the state of CR goes "high". IC35 is enabled when the state of CR is "low". The outputs of pins 12, 11, 9, and 8 are fed to the SELECT INPUT pins of ICs 30 through 34. The output of IC35 is also fed to the inputs of IC36, an open collector quad 2-input AND gate chip. A serial combination of LED and 220 ohm resistor at each gate output is used to display the current memory address position in hexadecimal. When the respective AND gate output goes "high", the current sunk through the LED to ground causes the LED to illuminate.

Figure 21 shows the schematic for the memory display circuit. ICs 37 through 41 are 7447 BCD-to-seven segment decoder/driver chips. With the state of ME "low" and WE "high", the data in permanent memory are non-destructively displayed by the Litronix 747 seven segment displays. The LED/resistor and display/resistor sections are located on the

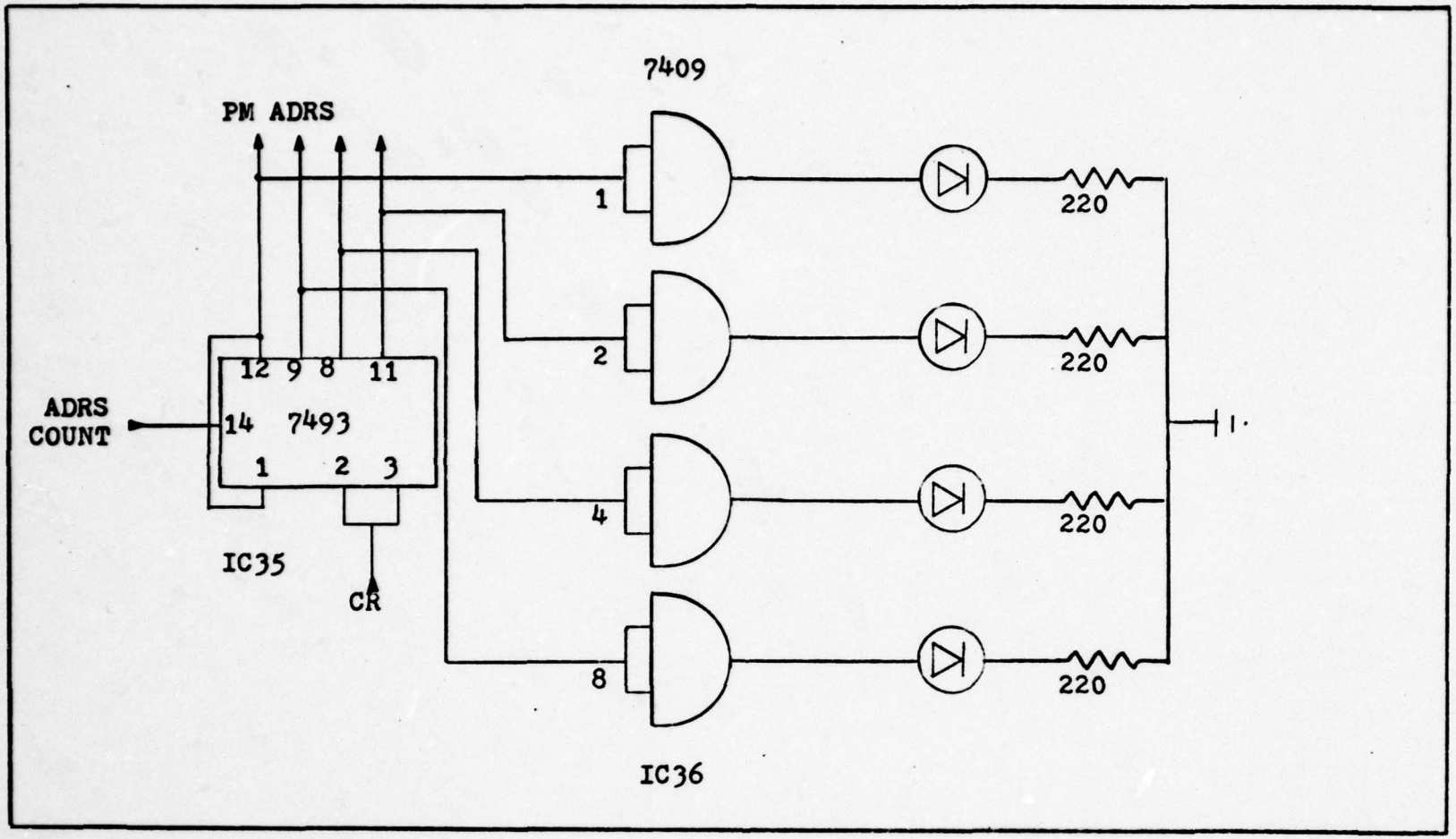

Figure 20. Schematic of the Address Count and Display Circuit.

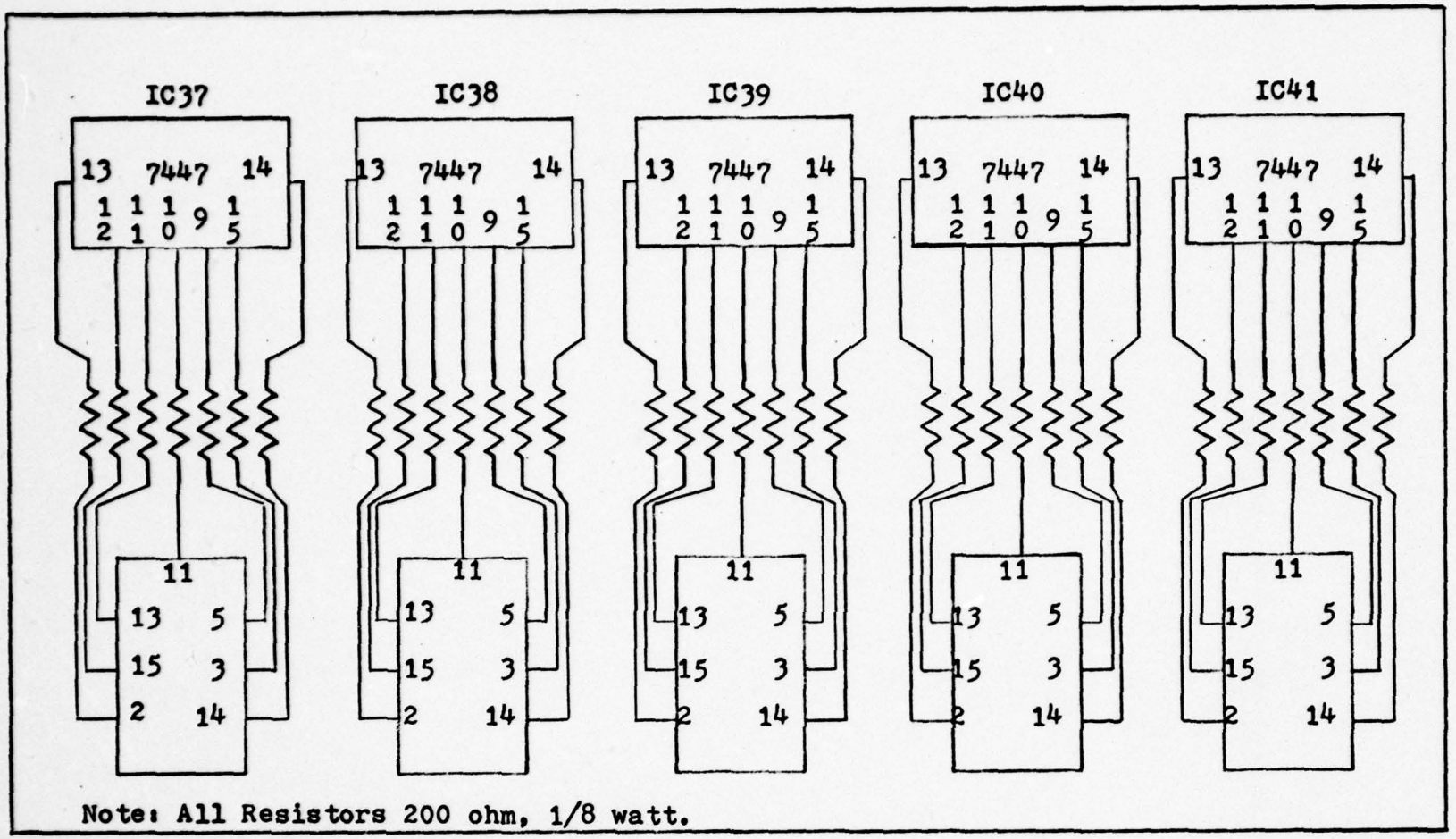

Figure 21. Schematic of Memory Display Citcuit.

display board mounted on the front panel of the electronics package.

Chassis and Component Layout

A BUD Tilt-A-View steel cabinet houses the system's electronics. The overall dimensions of the cabinet are 114.3mm high, 254mm deep, and 381mm wide. All system control inputs are accessed via the chassis front panel. Figure 22 shows a diagram of the front panel. Two BNC connectors, four monentary contact SPST switches, three ON-OFF-ON toggle switches, eight SPDT minature slide switches, and an indicator light are mounted on the front panel. Two 22mm x 63mm rectangular windows were cut to provide access to two sets SPDT bubble time filter slide switches (only one set is used in the final design). A 50mm x 118mm rectangular window provides access to the display board.

The upper BNC connector feeds the VCS signal to the video processing board. The lower BNC connector feeds the VDS signal also to the video processing board. Momentary contact switch 1 (DE) generates the data enable pulse. Momentary contact switch 2 sends the data enable flip-flop reset (RST) signal to the video processing board. Momentary contact switch 3 (PT) activates the drive field external pulse trigger circuit. READ/WRITE ENABLE and WE signals are generated by the left-center toggle switches. The bubble

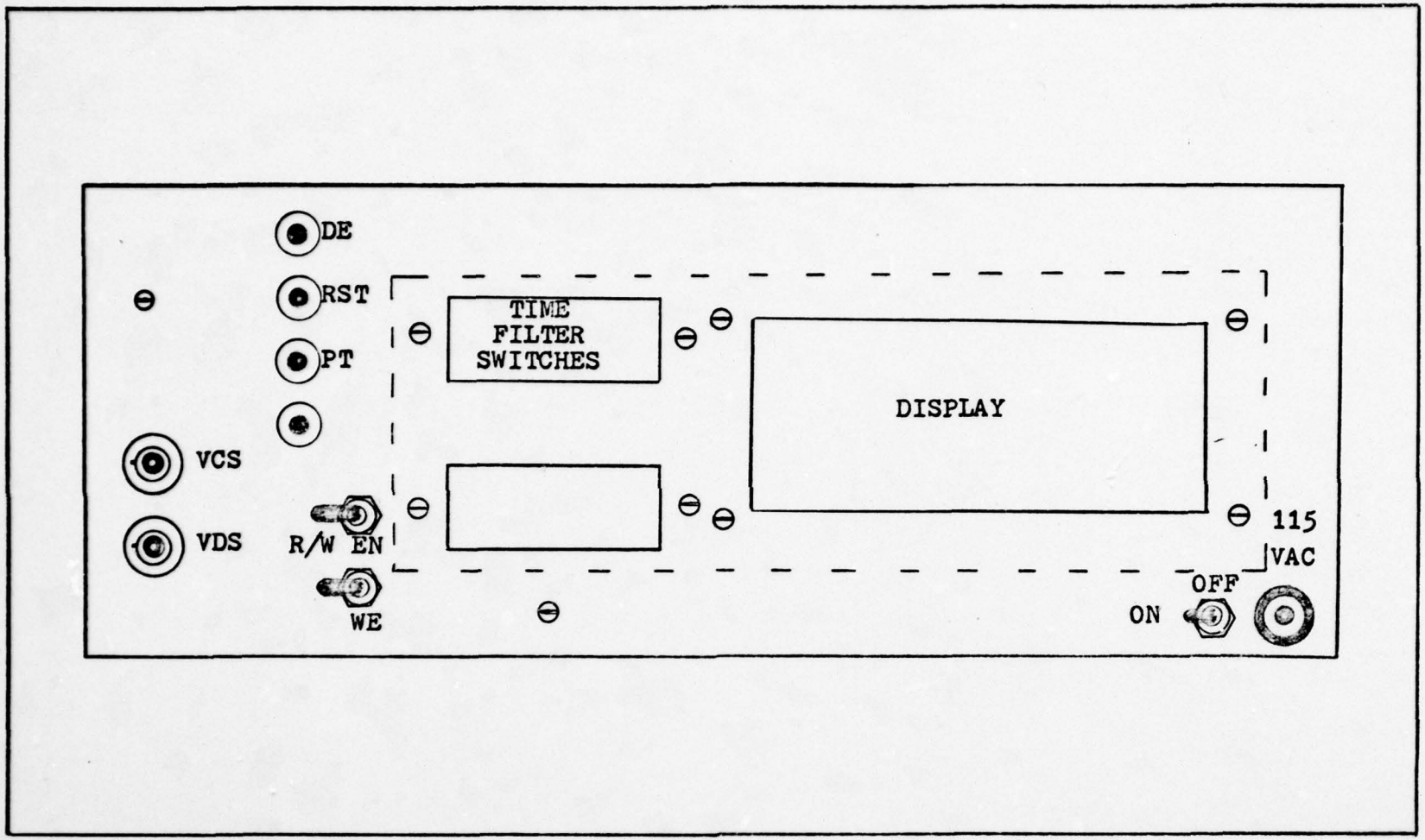

Figure 22. Front Panel of Electronics Package Cabinet.

time filter switch bank consists of 8 slide switches mounted on a piece of perforated board which mounts flush in the upper of the two small rectangular windows. The 61mm x 165mm display board is mounted behind the largest of the windows using four 6.4mm in diameter, tapped, 12.5mm long aluminum standoffs. Figure 23 shows the display board device placement. The ± 15 VDC power supply ON/ OFF toggle switch and indicator lamp are located on the lower right portion of the front panel.

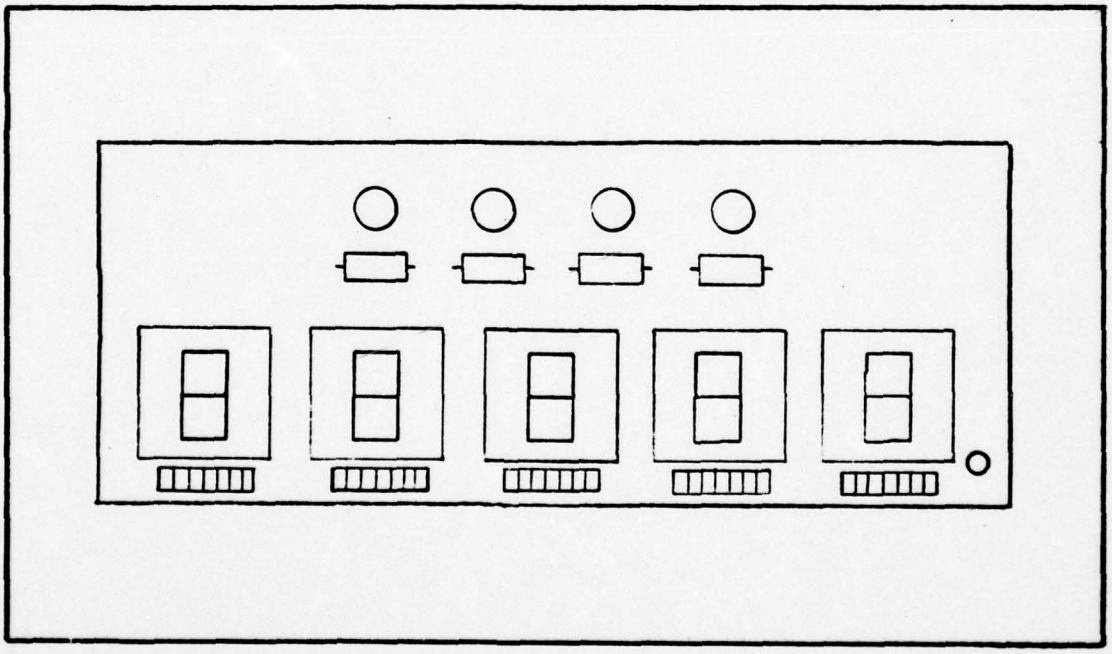

Figure 23. Display Board Device Placement.

Figure 24 shows the significant features of the chassis rear panel. Except for the internally mounted ± 15 VDC power supply, all other power requirements are satis-

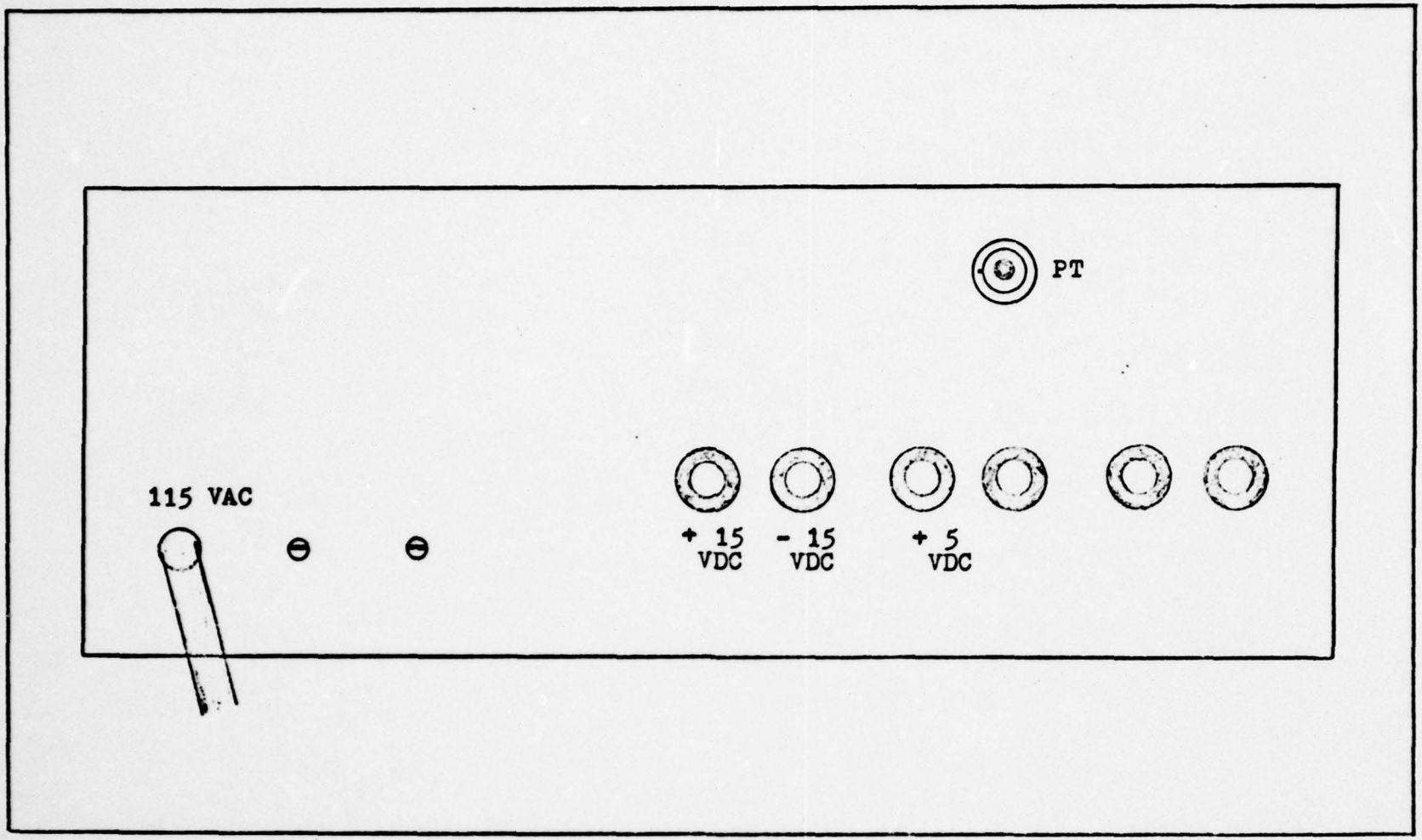

Figure 24. Rear Panel of Electronics Package Cabinet.

fied externally. Six banana plugs (three sets of two) provide either the measurement point or input for the ± 15 VDC and + 5 VDC power supplies. The BNC connector feeds the external trigger (PT) pulse to the E&H Model 123 pulse generator/amplifier. Transformer primary voltage for the internal power supply is obtained through the AC power cord.

Figures 25 and 26 show the placement of components on the video processing and memory boards (IC placement). Figure 27 shows the video processing, memory, and power supply board placement in the cabinet. The processing and memory boards are mounted using 32mm aluminum standoffs. The power supply is mounted using 12.5mm standoffs.

Data obtained from the electronics package are reduced to mobility values using a Hewlett-Packard 9825 minicomputer. The following chapter describes the data reduction program.

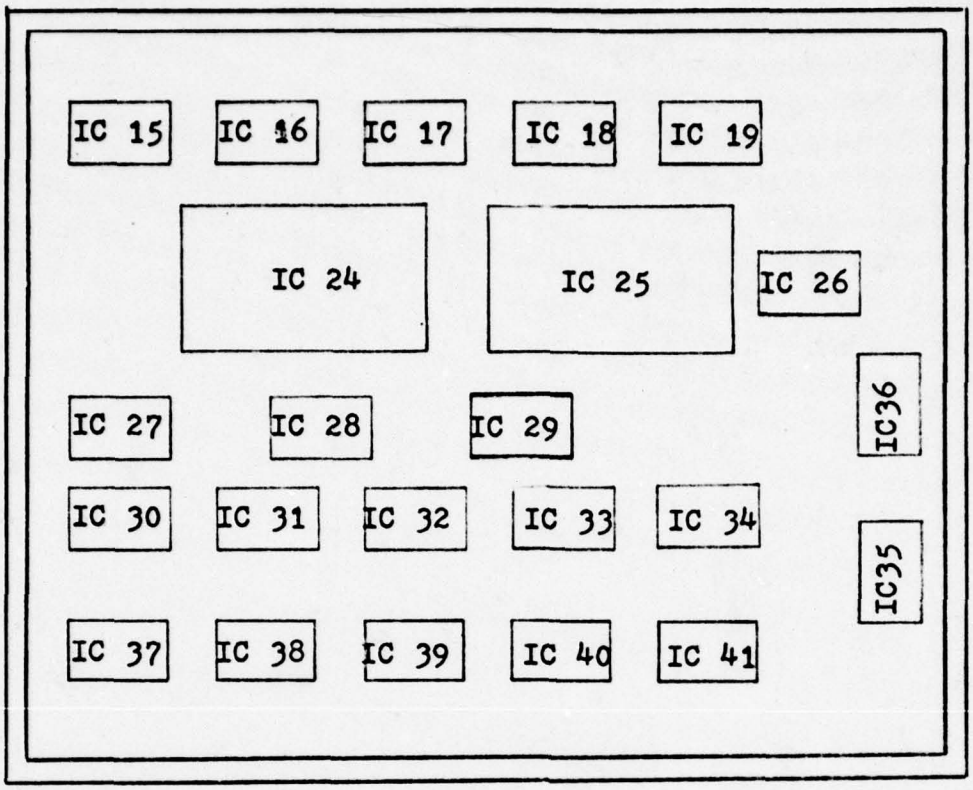

Figure 26. IC Placement on Memory Board.

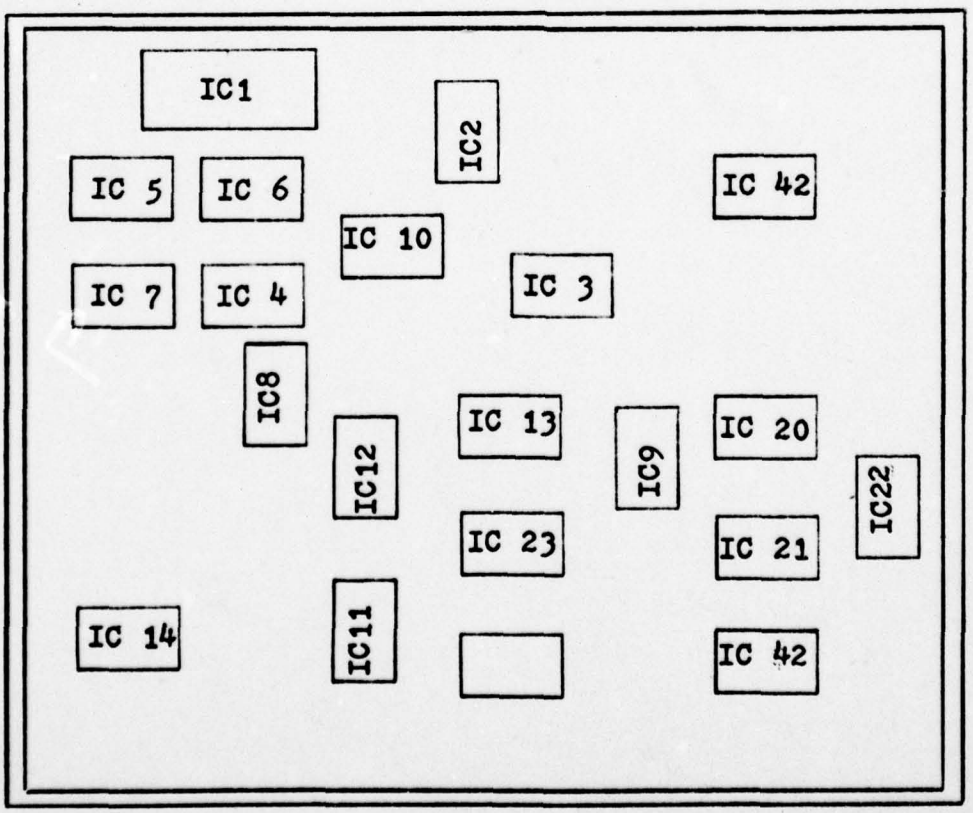

Figure 25. IC Placement on Video Processing Board.

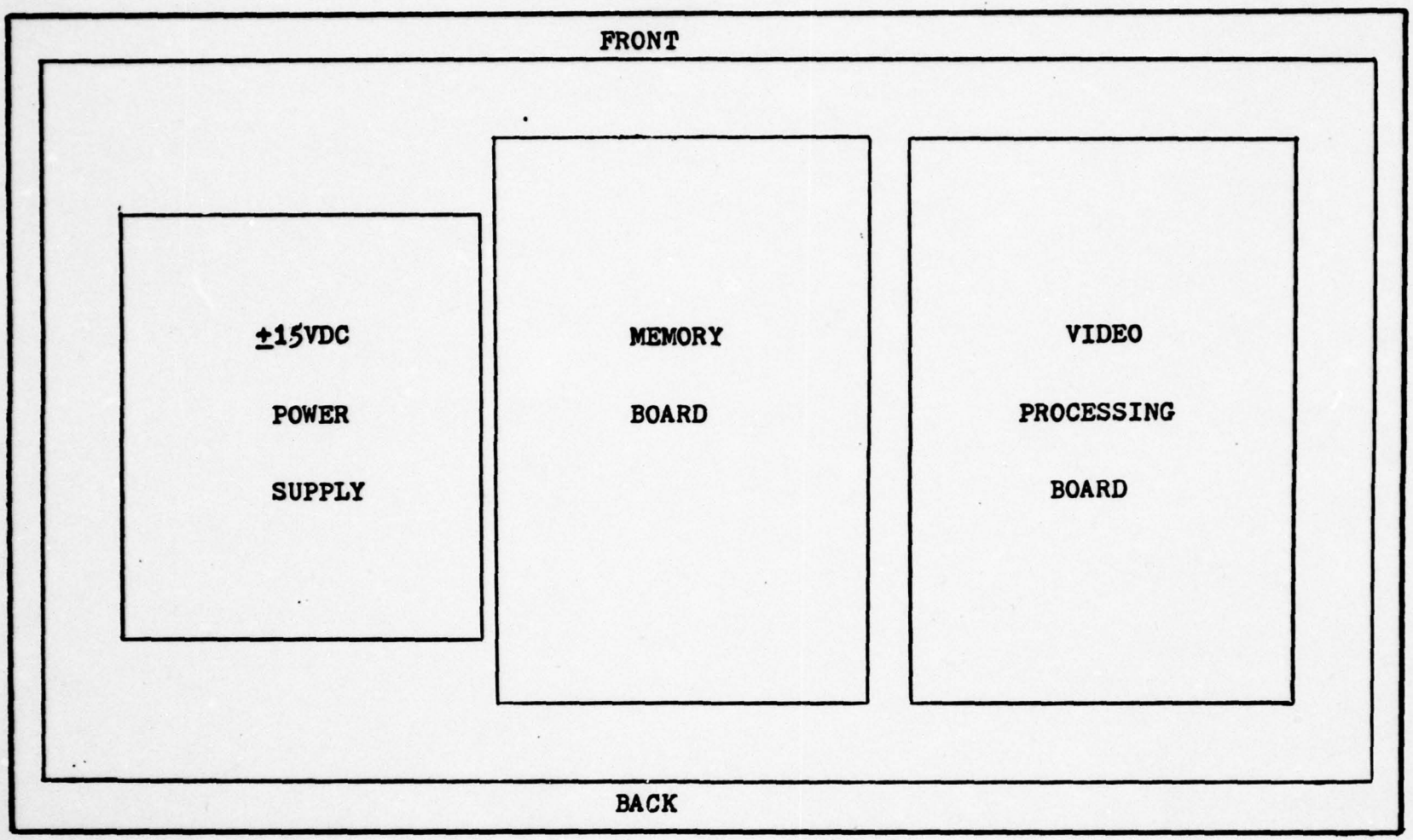

Figure 27. Cabinet Placement of Processing, Memory, and Power Supply Boards.

V. Mobility Computation Program

The purpose of this section is to describe the HP 9825-compatible mobility computation program. This program, written in HPL, calculates the domain mobility for a sample of garnet material using position data from the electronics section.

Overview

For this report, the linear mobility equation $V_x = u_x H$ (where u_x is the mobility) is used to derive a value for the domain mobility in a sample. Two equipment alignment constraints result from the method of calculation to be described. The video camera must be aligned very nearly parallel to the FOV horizontal axis. The drive field coil must be aligned very nearly parallel to the FOV vertical axis. A cartesian coordinate system results with the magnetic field gradient vector in the x-direction. Domain movement is referenced to the x-direction.

Data from the electronics section internal memory

(values of initial bubble temporal position (IBP) and final bubble temporal position (FBP)) are fed to the computer by the operator. The bubble filter setting, microscope field of view, CCTV horizontal line length, bias field coil strength, and CCTV vertical resolution are other parameters required by the program.

Mobility Program

A 16x16 array (E) is used as a temporary data operation/storage matrix. Variables O, F, H, B, and V are used to represent the bubble time filter setting in microseconds, microscope FOV in micrometers, CCTV horizontal line length in microseconds, bias field strength in gauss, and CCTV vertical resolution respectively. The columns of array E represent the following values:

column 1- IBPs from the electronics system memory in sequence;

column 2- FBPs from the electronics system memory in sequence;

column 3- Y coordinates of adjusted IBPs in micrometers;

column 4- X coordinates of adjusted IBPs in micrometers;

column 5- Y coordinates of adjusted FBPs in micrometers;

column 6- X coordinates of adjusted FBPs in micrometers;

column 7- Square of values for column 5 minus column 3;

column 8- Square of values for column 6 minus column 4;

column 9- Line segment lengths between respective FBPs and IBPs;

column 10- Mobility values with respect to the x-axis;

column 11- Domain translation angle of divergence from the x-axis.

Program statements 1 through 3 print an explanation of the program's purpose for the operator. Statements 4 through 8 print requests for the operator to feed the values for variables O, F, H, J, and V into the computer memory. Statements 9 through 22 provide the means for feeding the values for the domain IBPs and FBPs obtained using the electronics section into the computer memory. If the number of IBPs and FBPs differ, a statement "Number of IBPs and FBPs are different" is printed and the program aborts.

The actual mobility computation begins with statement 24. Because the microscope inverts the image, the scene viewed by the camera is inverted. The x=0 line is located along the FOV's left side. The actual y=0 line is located along the top of the FOV before the image inversion. By subtracting the IBP and FBP values (in microseconds) from 15,000 (value of the enable circuit monostable output), the

IBP and FBP y-coordinate values are translated to their true position. Since the x-coordinate is treated as a percentage of the horizontal FOV (by dividing the IBP and FBP values by the horizontal line length and treating the remainder as the x-coordinate), subtracting this percentage from 1 yields the actual IBP and FBP x-coordinates.

Statements 25 and 27 compute the true IBP and FBP y-coordinate values in micrometers and place this information in E[I,3] and E[I,5] respectively. Statements 26 and 28 compute the true IBP and FBP x-coordinate values in micrometers and place this information in E[I,4] and E[I,6] respectively. The magnitude of the vector connecting each domain's initial and final positions is calculated using the formula $\sqrt{X^2+Y^2}=$ R where Y, X, and R are the variables Q, R, and S respectively. The corresponding values in columns five and three of array E are subtracted; the results are then squared and stored in array E, column 7 (statement 29). The respective values in column six and four of E are subtracted and the results squared and stored in column 8 of E (statement 30). Statement 31 performs the square root of the sum of the squares and stores the values in column 9 of E. The x component of the mobility for each domain is stored in column 10. The bubble translation angle of divergence from the x-axis is calculated using the expression arctan (Y/X)= θ. Column 11 contains the values for θ.

The mobility for each domain is printed during the

calculation sequence for operator perusal via statements 34 and 36. Statements 37 and 38 compute the average mobility and angle of divergence for each set of data. These values are sent to the printer by statements 40 and 41.

Statements 42 through 45 allow the operator to feed another set of data into the computer with or without changing the values of O, F, H, B, and V. A listing of the computer program follows:

```
0: dim E 16,16
1: prt "This program calculates the mobility of a
   magnetic domain in"
2: prt "garnet material wth data from the mobility
   measurement system"
3: spc2
4: prt "Enter bubble filter setting in usecs";ent O;
   spc;prt O;spc2
5: prt "Enter FOV in micrometers";ent F;spc;prt F;
   spc2
6: prt"Enter CCTV horizontal line length (usec)";ent H;
   spc2
7: prt "Enter bias field strength (gauss)";ent B;spc;
   prt B;spc2
8: prt "Enter CCTV vertical resolution";ent V.spc;prt V;
   spc2
9: prt "Input IBP values in sequence";spc
10: prt "STORAGE LIMITED TO 16 VALUES";spc
11: prt " If no. of points  16,type in 0 after last
```

```
    entry";spc2
12: for I=1 to 16;prt "Enter point no.",I;spc;ent L
13: if L=0;gto 16;prt L;spc2
14: L-0/2 → E[I,1]
15: next I
16: I-1 → M;Ø → I;Ø → P
17: prt "Input FBP points in sequence";spc2
18: prt "DATA STORAGE LIMITED TO 16 POINTS";spc
19: prt "If no. of points  16,type in Ø for last entry"
    ;spc2
20: for J=1 to 16;prt "Enter point no.",J;spc;ent K;
21: if K=Ø;gto 23;prt K;spc2;K-0/2 → E[I,2]
22: next J
23: J-1 → J;if J=M;gto 24;prt "Number of IBPs and FBPs
    are different";end
24: for I=1 to M
25: int(((15ØØØ-E[I,1])/H)+1)*2*F/V → E[I,3]
26: (1-((((15ØØØ-E[I,1])/H)+1)-int(((15ØØØ-E[I,1])/H)
    +1)))*F → E[I,4]
27: int(((15ØØØ-E[I,2])/H)+1)*2*F/V → E[I,5]
28: (1-((((15ØØØ-E[I,2])/H)+1)-int(((15ØØØ-E[I,2])/H)
    +1)))*F - E[I,6]
29: E[I,5]-E[I,3] → Q;Q↑2 → E[I,7]
30: E[I,6]-E[I,4] → R;R↑2 → E[I,8]
31: Q↑2+R↑2 → S;√S → E[I,9]
32: √S*cos(atn(Q/R))/B → E[I,10];atn(Q/R) → E[I,11]
33: next I
```

```
34: prt "The mobility and angle of divergence for each
    point are as follows:";spc2
35: for I=1 to M
36: prt "Mobility (x-direction)= ",E[I,10] ;prt "Angle
    of Divergence = ",E[I,11] ;spc
37: E[I,10] +U → U
38: E[I,11] +W → W
39: next I
40: prt "The average domain mobility for these points
    is ",U/M;spc2
41: prt "The average angle of divergence for these
    points is ",W/M;spc2
42: prt "Want another iteration? Yes,type 1;No,type Ø";
    ent P
43: if P=Ø;gto 46
44: Ø → P;prt "Need to change O,F,H,B,V? If yes,type 1;
    no,type Ø";ent P
45: if P=1;gto 4;gto 9
46: end
```

VI. Results, Conclusions, and Recommendations

The results, conclusions, and recommendations of this report are presented in this chapter.

Results

Mobility Stage. The bias field coil required slight modification before the stage became compatible with the Ultraplot 3B microscope. The travel distance for the microscope objective lens was not sufficient to permit using the 40x objective lens (required for bubble work). This was caused by failure to compensate for the additional 4 millimeters milled from the 38.1mm circular area in the specimen holder. Alleviation of this problem required the bias coil to be reduced in thickness by 6mm. A request to the AFIT shops for fabrication of a new coil form has been forwarded. It is projected that sufficient field strength (160 gauss is required for 2um bubble work) will be available from the new coil without any heat problems.

Electronics Section. All circuitry in the electronics

section was fabricated and verified as functioning as designed. System checkout was accomplished using simulated bubble video information. By mounting a piece of black cardboard was a pin hole in the center over the camera lens, a single domain was simulated. By varying the light intensity and the f-stop of the camera, the minimum contrast difference for successful detection by the video processing section was established. With the reference voltage level set at 0.6 volts and the voltage difference between the black level and the "pseudo" domain at 0.7 volts, signal widths of less than 2 usecs were processed by the time filter circuitry. Two microseconds in time equates to about 1/25 the horizontal line width for a 400 line camera. Setting the reference voltage level at less than 0.6 volts resulted in false triggering due to the noise level in the circuit. Noise sources and amplitudes measured in the circuit are the video camera at 0.3 volts (10 MHz cyclic), the +5 VDC power supply at 0.3 volts, and the ± 15 VDC op amp power supply at 0.5 volts. A low pass non-inverting filter inserted between the VCS input and the comparator input effectively negated the noise from the video camera. An attempt to lower the ± 15 VDC power supply noise using a Hewlett Packard dual 0-20 volt, 0.75 ap power supply in lieu of the internal supply resulted in noise levels approaching 1.0 volts. At this noise level, the electronics section is rendered useless. Thus the video processing circuitry required the incoming VCS to exhibit voltage difference greater than o.7 volts for successful operation.

The use of an operational amplifier in the VCS processing circuit required the insertion of the same component in the VDS processing circuit to minimize any time delays between the circuits' outputs. The use of a 4x inverting low pass filter between the VDS input and the vertical enable pulse generator (IC8) resulted in the successful generation of signal E with minimum noise effects and delay between the VCS and VDS outputs.

The Telemation video camera was not available due to a malfunction. A RCA CT1005 camera was substituted. The CT1005 is a general purpose, vidicon equipped camera. Using a 10x eyepiece equipped microscope attachment tube, the camera was mounted on the microscope. A sample of RCA 12 micrometer bubble material was used to obtain a realistic measurement of the domains' contrast differences. The microscope's cesium iodide light source was used for illumination.

With the cross-polarizers set to cancel the anti-parallel domain transmission, the resulting contrast difference was not sufficient for observation of the domain on an oscilloscope. A contrast difference on the order of 0.1 volt was obtained. If the contrast differences from a 12 micrometer material were not sufficient for discrimination, the same can be said for 2 and 5 micrometer materials.

The amount of light transmitted by the domains (both parallel and antiparallel) can be approximated. The amount of rotation of the plane of polarization of lineraly polarized light is proportional to the magnetic induction (bias

field strength) and the length of travel through the material. A typical figure for the amount of rotation per centimeter of travel distance for Sm amd Eu doped garnet materials is 5000 degrees/centimeter. For 2 and 5 micrometer domain materials (2 and 5 micrometer thick materials), the angle (θ) that results between the parallel domain rotated plane of polarization and the antiparallel domain rotated plane of polarization is equal to twice the thickness of the material times 5000 degrees/centimeter. These angles are on the order of 4 and 10 degrees respectively. With the cross-polarizers set to cancel the antiparallel domain transmission, the light intensity from the parallel domain transmission is equal to $I\cos^2(90-\theta)$ where I is the intensity of the incoming (incident) illumination. Given information on the microscope illumination source wavelength and intensity, losses in the system due to absorption by the optics, and information on the vidicon input/output, it should be possible to calculate the voltage contrast difference for a given sample of material and thus establish whether the VCS signal is sufficient without some form of preprocessing. Apparently some commercial firms (Sperry for example) use image intensifier tubes between the camera and the microscope to preprocess the video contrast signal. In order to achieve the necessary 0.7 volt contrast difference required by the video processing circuit, this type of setup appears mandatory in light of the measurements

taken on the 12um material. Use of the Telemation camera alone would probably not be sufficient.

Mobility Program. All syntax and computational errors were removed from the mobility computation program. Imaginary IBPs and FBPs were fed into the program to check the correctness of the computational logic. Because of the inability to obtain actual bubble position data, no actual mobility computations were done.

Conclusions

1. It is feasible to construct a fully automated domain mobility measurement system based on the results obtain during this study. The system constructed in this report was sophisticated enough to demonstrate this.

2. Use of an image intensifier device is necessary to obtain processable contrast differences between parallel and antiparallel domains.

3. The video processing circuit in this report needs to be redesigned and properly shielded. In addition, low noise DC power supplies (possibly batteries) should be used to alleviate the noise problem. The electronics section operates on + 5VDC at 2 amps and ± 15VDC at 200 ma.

4. It would be more cost effective to implement the fully automated system with a microprocessor in lieu of the HP 9825.

Recommendations

This method of mobility measurement has several failings. A less automated system based on the work of Humphrey (see reference 1) would alleviate the failings of the fully automated system. These failings are as follows:

Static measurement of a dynamic parameter;

Difficulty in matching IBP and FBP;

Requirement for pre-test manipulations to assure the no domains exit the FOV during application of the drive field.

The ultra high speed laser flash photographic technique would require the operator to feed the data into the computer. This could easily be accomplished using the digitizer attachment on the 9825.

This semi-automatic technique would have the following advantages:

1. A dynamic measurement system measuring a dynamic parameter;

2. A permenent multi-exposure record of each domain's track so that mobility during the displacement period could be measured;

3. No problem matching IBPs and FBPs;

4. Little worry about having to pre-process the

samples to assure that the domains would not exit the FOV.

I would recommend that this technique be pursued in addition to further pursuance of the fully automated system.

Bibliography

1. Kobayashi, Tsutomu, Peter K. George, and Floyd B. Humphrey. "Dynamics of Bubbles in Field Access Devices Studied Using a High Speed Optical Sampling Microscope." IEEE Transactions on Magnetics, Vol.Mag-12,No. 3: 202-208 (May 1976).

Vita

Richard Leo Eilers was born on 1 August 1951, in St. Louis, Missouri, the son of Charles M. and Betty J. Eilers. He graduated in 1969 from Grover Cleveland High School in St. Louis, Missouri. After four dubiously wonderful years in the Colorado foothills, he received a Bachelor of Science degree in Electrical Engineering and a regular Air Force commission from the United States Air Force Academy. Following a medical removal from undergraduate pilot training he spent two and one half years as a Wing Electromagnetic Environment Test Engineer with the 3246 Test Wing at Eglin Air Force Base, Florida. He is the author of several technical reports and papers in the area of radar and electronic warfare.

He is a member of IEEE, ETA KAPPA NU, and TAU BETA PI.

He is married to the former Barbara Sue Ham of Auburn, Alabama.

Permanent Address: 4173 Tholozan Ave.
St. Louis, Missouri 63116

UNCLASSIFIED

SECURITY CLASSIFICATION OF THIS PAGE (When Data Entered)

REPORT DOCUMENTATION PAGE	READ INSTRUCTIONS BEFORE COMPLETING FORM
1. REPORT NUMBER: AFIT/GE/EE/78-1	GOVT ACCESSION NO. / 3. RECIPIENT'S CATALOG NUMBER
4. TITLE (and Subtitle): An AUTOMATIC MAGNETIC BUBBLE MOBILITY MEASUREMENT SYSTEM EMPLOYING VIDEO PROCESSING.	5. TYPE OF REPORT & PERIOD COVERED: Master's thesis, ~~MS Thesis~~ / 6. PERFORMING ORG. REPORT NUMBER
7. AUTHOR(s): Richard L. Eilers, ~~Capt, USAF~~ Leo	8. CONTRACT OR GRANT NUMBER(s)
9. PERFORMING ORGANIZATION NAME AND ADDRESS: Air Force Institute of Technology (AFIT-EN) Wright-patterson AFB, Ohio 45433	10. PROGRAM ELEMENT, PROJECT, TASK AREA & WORK UNIT NUMBERS
11. CONTROLLING OFFICE NAME AND ADDRESS: Electronics Research Branch (AFAL-DHR) Air Force Avionics Laboratory WPAFB, OHIO 45433	12. REPORT DATE: Mar [redacted]78 / 13. NUMBER OF PAGES: 75 [redacted]
14. MONITORING AGENCY NAME & ADDRESS (if different from Controlling Office)	15. SECURITY CLASS. (of this report): Unclassified / 15a. DECLASSIFICATION/DOWNGRADING SCHEDULE

16. DISTRIBUTION STATEMENT (of this Report)

Approved for public release; distribution unlimited

17. DISTRIBUTION STATEMENT (of the abstract entered in Block 20, if different from Report)

18. SUPPLEMENTARY NOTES

Approved for public release; IAW AFR 190-17

Jerral F. Guess, Captain, USAF
Director of Information

19. KEY WORDS (Continue on reverse side if necessary and identify by block number)

Magnetic Domains
Mobility
Mobility Measurement

20. ABSTRACT (Continue on reverse side if necessary and identify by block number)

A semi-automatic bubble mobility measurement system emplcying a Zeiss Ultraplot 3B microscope, video camera, and processing circuitry was designed and constructed. The method of measurement was static in nature i.e. measurement of the pre and post-drive domain positions.

DD FORM 1 JAN 73 1473 EDITION OF 1 NOV 65 IS OBSOLETE

UNCLASSIFIED

SECURITY CLASSIFICATION OF THIS PAGE (When Data Entered)

012225

kc

A two piece mobility stage was constructed. The stage base incorporated a removable bias field coil capable of generating a 160 gauss field with little heat generation. The brass specimen holder contains the drive field coil. An E&H 123 pulse generator/amplifier provides the 50 volt, one microsecond drive field current pulse.

The electronics section converts the domain's light contrast difference in the microscope to a voltage difference in time. Voltage contrast differences of 0.7 volts and domain wifths of 2us are required to achieve discrimination.

A HP 9825 compatible mobility computation program was written and debugged. This program calculated the domain mobility based on displacement measured by the electronics section.

Simulated domain contrast differences were used to validate the system.